Appendix E
FCT Document Cover Sheet

Name/Title of Deliverable/Milestone	Post-Irradiation Examination of Zircaloy-4 Samples in Target Capsules HYCD-1 and HYCD-2
Work Package Title and Number	ST Storage and Transportation Experiments FT-13OR080504
Work Package WBS Number	1.02.08.05
Responsible Work Package Manager	Rob Howard
	John M. Scaglione (Name/Signature) for R. Howard

Digitally signed by John M. Scaglione
DN: cn=John M. Scaglione, o=Reactor and Nuclear Systems Division, ou=DSSI, email=ScaglioneJM@ornl.gov, c=US
Date: 2013.03.28 11:01:24 -04'00'

Date Submitted 3/28/2013

Quality Rigor Level for Deliverable/Milestone	☐ QRL-3	☐ QRL-2	☐ QRL-1 ☐ Nuclear Data	☒ N/A*

This deliverable was prepared in accordance with Oak Ridge National Laboratory
(Participant/National Laboratory Name)

QA program which meets the requirements of
☒ DOE Order 414.1 ☐ NQA-1-2000

This Deliverable was subjected to:

☒ Technical Review ☐ Peer Review

Technical Review (TR)	**Peer Review (PR)**
Review Documentation Provided	**Review Documentation Provided**
☐ Signed TR Report or,	☐ Signed PR Report or,
☐ Signed TR Concurrence Sheet or,	☐ Signed PR Concurrence Sheet or,
☒ Signature of TR Reviewer(s) below	☐ Signature of PR Reviewer(s) below

Name and Signature of Reviewers

John Scaglione John M. Scaglione

Digitally signed by John M. Scaglione
DN: cn=John M. Scaglione, o=Reactor and Nuclear Systems Division, ou=DSSI, email=ScaglioneJM@ornl.gov, c=US
Date: 2013.03.28 11:01:47 -04'00'

*Note: In some cases there may be a milestone where an item is being fabricated, maintenance is being performed on a facility, or a document is being issued through a formal document control process where it specifically calls out a formal review of the document. In these cases, documentation (e.g., inspection report, maintenance request, work planning package documentation or the documented review of the issued document through the document control process) of the completion of the activity along with the Document Cover Sheet is sufficient to demonstrate achieving the milestone. QRL for such milestones may be also be marked N/A in the work package provided the work package clearly specifies the requirement to use the Document Cover Sheet and provide supporting documentation.

Post-Irradiation Examination of Zircaloy-4 Samples in Target Capsules HYCD-1 and HYCD-2

Y. Yan
R. H. Howard
L. J. Ott

Project Manager
R. L. Howard

Used Fuel Disposition Campaign

March 2013

Post-Irradiation Examination of Zircaloy-4 Samples in Target Capsules HYCD-1 and HYCD-2

Y. Yan, R. H. Howard, L. J. Ott

Project Manager
R. L. Howard

Oak Ridge National Laboratory

March 2013

CONTENTS

LIST OF FIGURES

Page

LIST OF FIGURES (continued)

Page

LIST OF TABLES

1. INTRODUCTION

Normal operation of nuclear fuel in a reactor results in the formation of a waterside corrosion layer (oxide) and the introduction of hydrogen into the zirconium cladding via the reaction $2H_2O + Zr \rightarrow ZrO_2 + 4H$. With increasing corrosion, the hydrogen concentration in the cladding will exceed its terminal solid solubility and brittle zirconium hydrides ($Zr + 2H \rightarrow ZrH_2$) may precipitate as cladding cools, which causes cladding ductility and failure energy to decrease.[1,2,3] The weakened cladding, degraded due to hydride precipitates, increases the likelihood of failure during very long-term storage and/or transportation of used nuclear fuel (UNF).

The DOE Used Fuel Disposition Campaign (UFDC) has tasked Oak Ridge National Laboratory (ORNL) to investigate the behavior of light-water-reactor fuel cladding material performance related to extended storage and transportation of used fuel. Fast neutron irradiation of pre-hydrided zirconium-alloy cladding in the High Flux Isotope Reactor (HFIR) at elevated temperatures has been used to simulate the effects of high burnup on used fuel cladding for use in understanding the materials properties relevant to very long-term storage (VLTS) and subsequent transportation. The irradiated pre-hydrided metallic materials will generate baseline data to benchmark hot-cell testing of high-burnup used fuel cladding. More importantly, samples free of alpha contamination can be provided to the researchers who do not have hot cell facilities to handle highly contaminated high-burnup used fuel cladding to support their research projects for the UFDC.

In order to accomplish this research, ORNL has produced unirradiated zirconium-based cladding tubes with a various known hydrogen concentration. Four capsules (HYCD-1 to HYCD-4) contained 3.0 in. (7.62 cm) to 6.0 in. (15.24 cm) hydrided zirconium-based samples (0.374 in. outer diameter [OD]) were inserted in HFIR for neutron irradiation in HFIR Cycle 440B. HYCD-1 was removed after one irradiation cycle (440B) and HYCD-2 after three irradiation cycles (442). The purpose of this progress report is to summarize the work that has been performed so far on HYCD-1 and HYCD-2.

2. SPECIMEN PREPARATION

2.1 DESCRIPTION OF CLADDING MATERIALS

As-fabricated 17×17 Zry-4 and ZIRLO cladding alloys were provided to ORNL by Sandia National Laboratory. For the cladding alloys received by ORNL, measurements were performed to determine the OD, wall thickness and chemical composition. Table 2.1 summarizes the dimensions and measured chemical composition of the Zry-4 and ZIRLO used in the ORNL test program, along with nominal composition of commercial Zircaloy-4 cladding. The tin content of our specimens is lower than the nominal composition of commercial Zircaloy-4.

Table 2.1. Dimensions and chemistry of Zry-4 and ZIRLO used in the ORNL test program (the "<" sign means below the detection limit)

Parameter	Zircaloy-4[a]	17×17 Zircaloy-4	17×17 ZIRLO
OD (mm)	---	9.50	9.50
Wall thickness (mm)	---	0.57	0.57
Sn (wt %)	1.45	1.26	0.97
Nb (wt %)			0.98
O (wt %)	0.125	0.13	0.12
Fe (wt %)	0.21	0.22	0.08
Cr (wt %)	0.10	0.10	---
S (wppm)			<10
C (wppm)			90
N (wppm)			50
H (wppm)		10	12
Zr	Balance	Balance	Balance

[a]ASTM B811 for nominal composition of commercial Zircaloy-4 cladding.

2.2 HYDROGEN CHARGING

Samples for hydriding were prepared by chemical etching in an acid blend of 49.5% nitric 49.5% hydrogen peroxide and 1% hydrofluoric acid, and were then cleaned (ultrasonic baths of RT ethanol and water). The target hydrogen concentrations range from tens of wppm to a few hundreds of wppm.

The Zr cladding samples were hydrogen charged by gaseous method at high temperature.[4,5] The hydriding system used for hydrogen loading in this report is shown in Fig. 2.1. It consists of a furnace that is heated to 400-450°C in the presence of hydrogen to introduce a desired quantity of hydrogen into the sample.[6] The chamber was evacuated (up to three times to ≈30 mm Hg below atmospheric pressure) before being filled with the charging gas, 96% Ar 4% H_2, to reduce oxidation of the surface of the cladding. The temperature, charging gas flow rate, and test duration were optimized to achieve the desired hydrogen concentration. The samples were then cooled in the furnace in a pure argon environment. A typical temperature profile used for hydrogen charging is shown in Fig. 2.2. After the hydrogen charging process, the sample surface is often slightly discolored, as shown in Fig. 2.3. A new static hydriding system (see Fig. 2.4) was recently developed at ORNL, by which the hydrogen loading is more predictable. Specimens used for HYCD-4 or afterwards were fabricated using the new hydriding system.

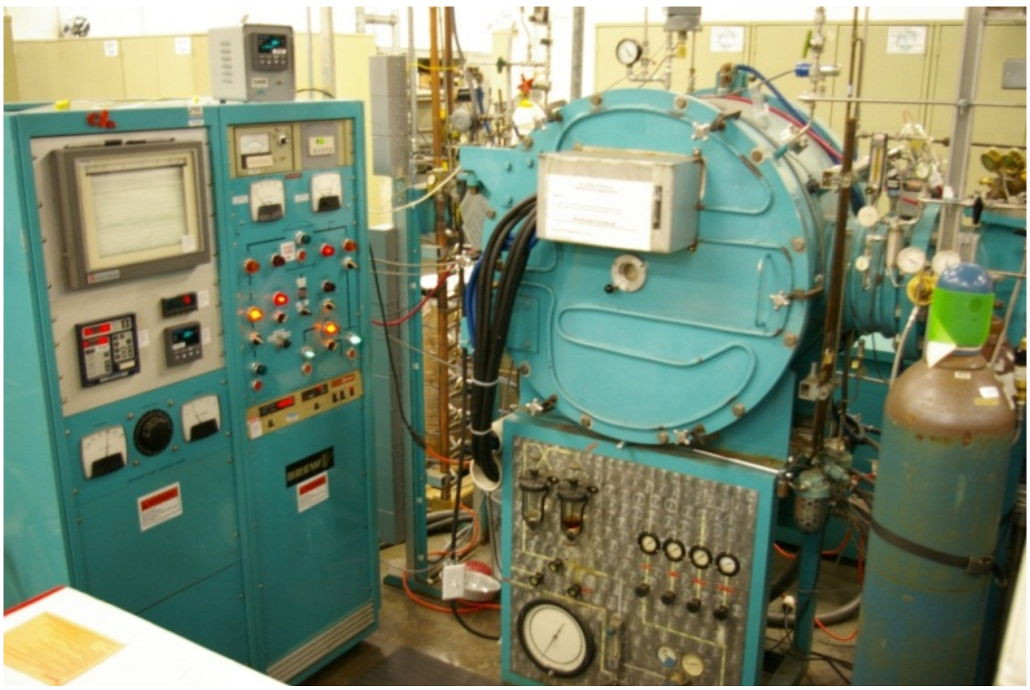

Fig. 2.1. The 901 Brew Furnace for hydrogen doping.

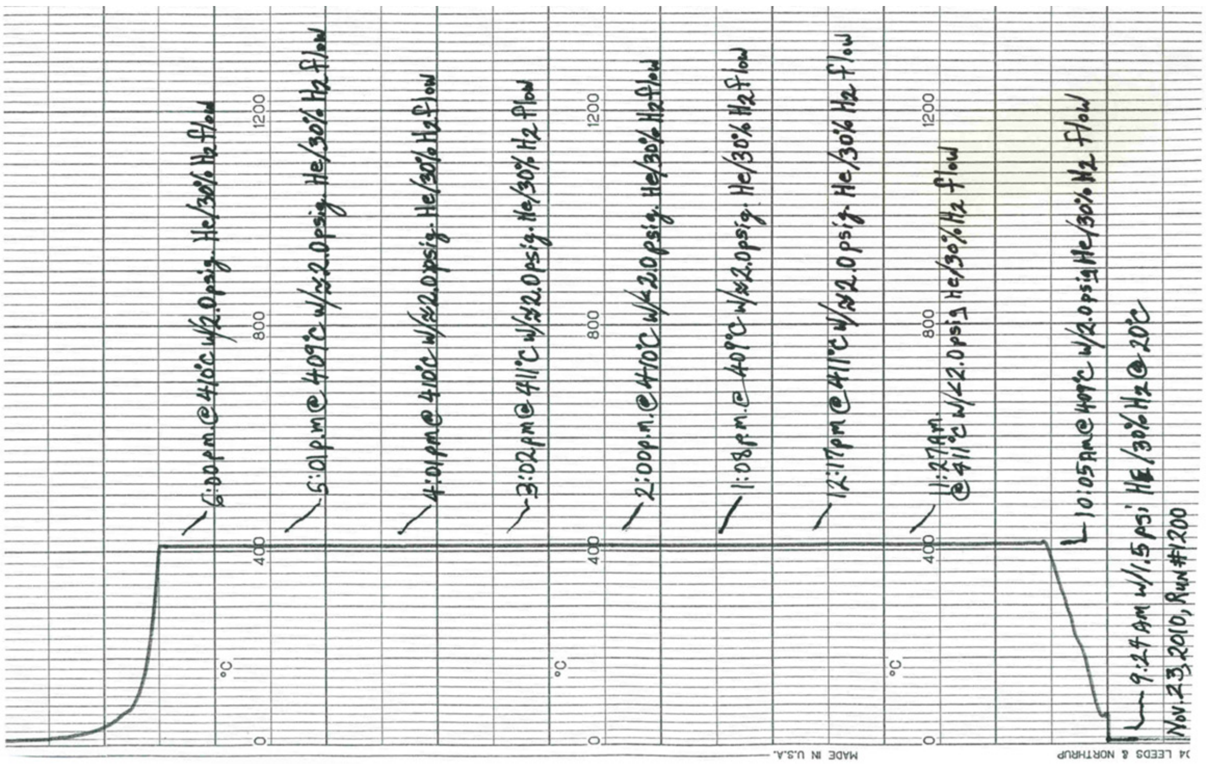

Fig. 2.2. Temperature profile for hydriding cladding materials.

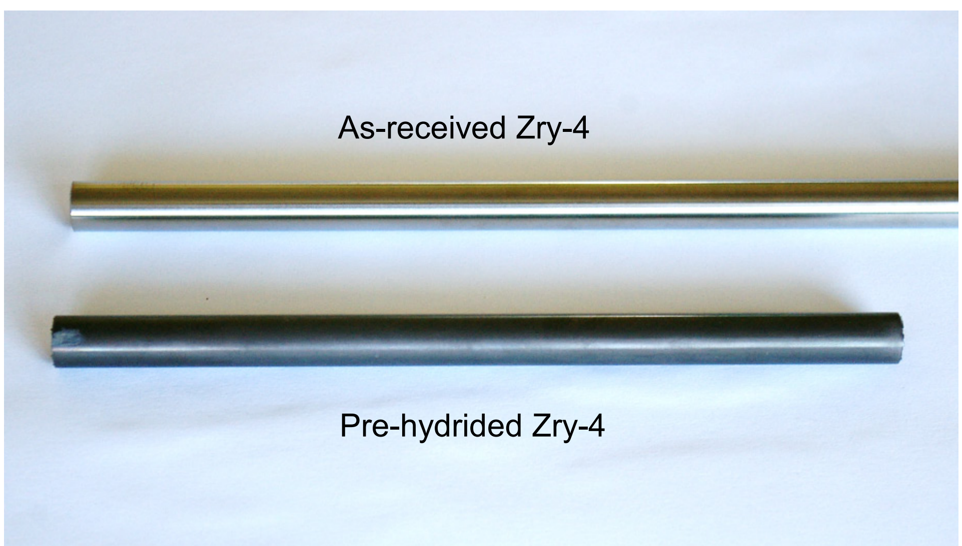

Fig. 2.3. Hydrided Zry-4 showing surface discolor.

Fig. 2.4. New static hydriding system.

2.3 CHARACTERIZATION OF HYDRIDED ZIRCALOY-4 SPECIMENS

The hydrogen content of the hydrided specimens was measured using the Vacuum Hot Extraction technique per ASTM E146-83. A LECO RH-404 Hydrogen Analyzer was used for hydrogen analysis, as shown in Fig. 2.5. The equipment is verified with standards of known hydrogen content before each testing. Under optimized test conditions, a relatively uniform hydrogen distribution along the axial direction was obtained (see Fig. 2.6). However, it is challenging to have repeatable results of hydrogen doping with the 901 Brew Furnace. The new static system Fig. 2.4 was developed to improve material hydriding.

Metallographic examinations were performed on hydrided Zircaloy-4 samples. Although axial gradients in hydrogen content are generally observed in hydrided Zircaloy-4 samples, our hydriding procedure resulted in uniform distribution of circumferential hydrides across the Zircaly-4 wall. As shown in Figs. 2.7-2.10, the hydride density increases as the hydrogen concentration in the sample increases. The measurements indicated the hydrogen contents of the specimens shown in Figs. 2.7-2.10 are from 70 to 790 wppm.

Fig. 2.5. LECO RH-404 Hydrogen Analyzer used for determining the hydrogen content.

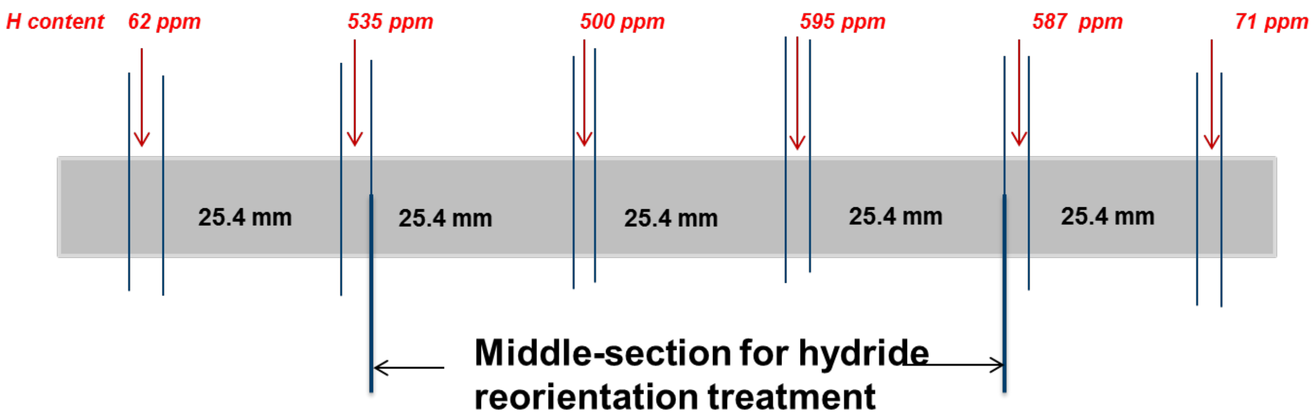

Fig. 2.6. Hydrogen distribution for pre-hydrided Zry-4 sample at 400°C for 8 hours with mixed gases of hydrogen and argon.

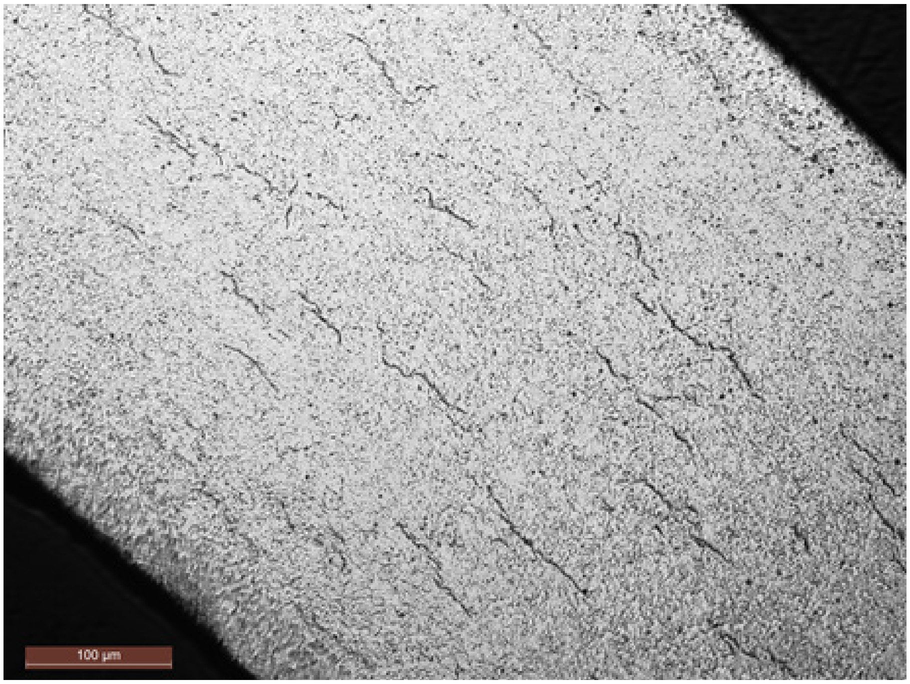

Fig. 2.7. Micrographs showing hydride distributions in hydrogen charged Zircaloy-4 of this study. The average hydrogen content of this location is ≈70 wppm.

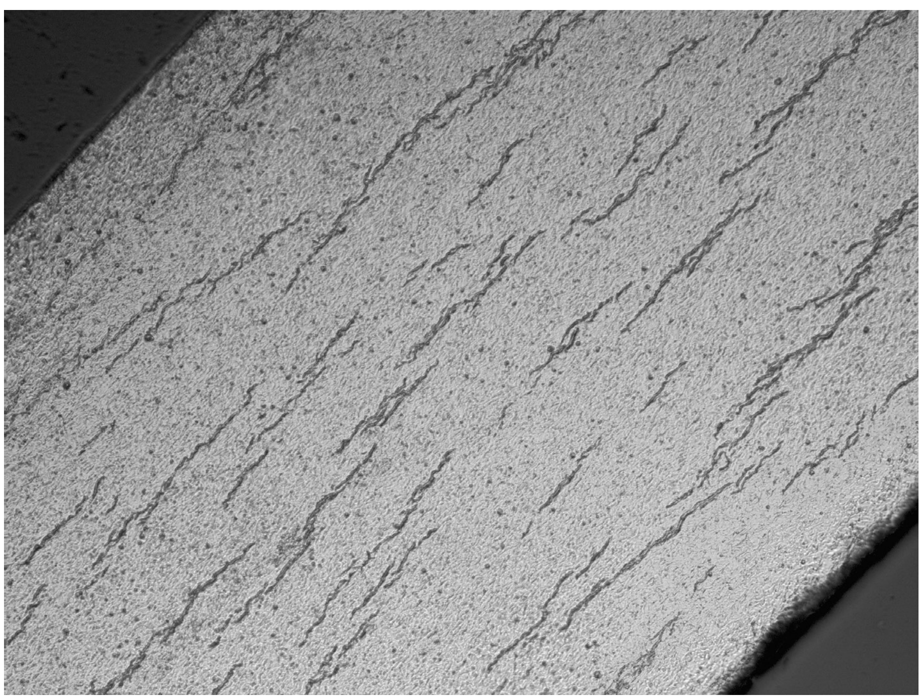

Fig. 2.8. Micrographs showing hydride distributions in hydrogen charged Zircaloy-4 of this study. The average hydrogen content of this location is ≈150 wppm.

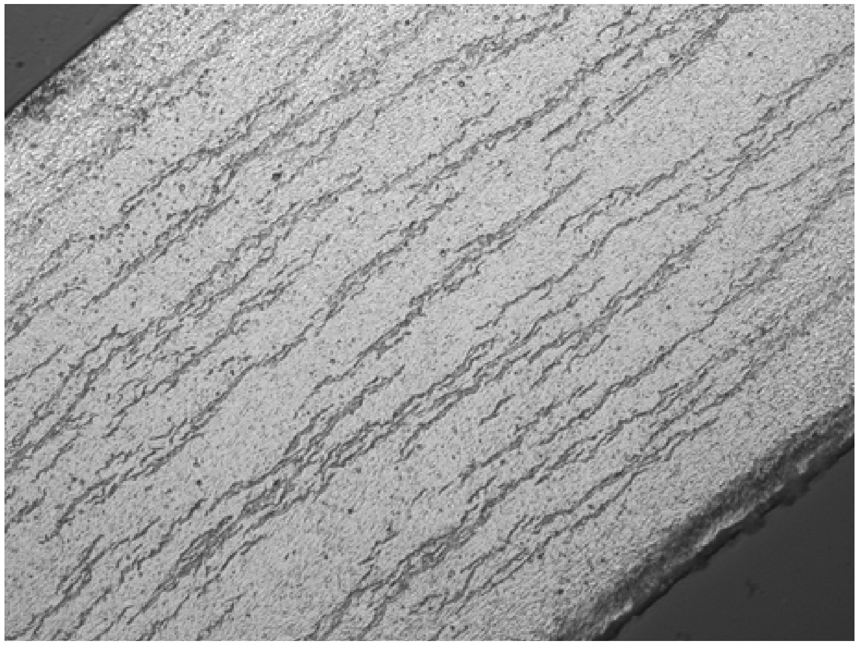

Fig. 2.9. Micrographs showing hydride distributions in hydrogen charged Zircaloy-4 of this study. The average hydrogen contents of this location is ≈320 wppm.

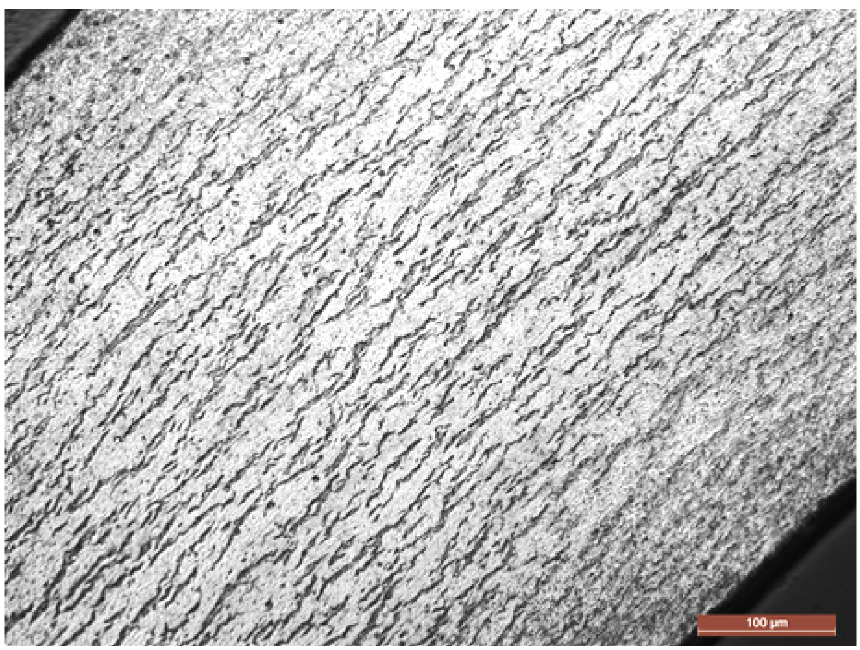

Fig. 2.10. Micrographs showing hydride distributions in hydrogen charged Zircaloy-4 of this study. The average hydrogen contents of this location is ≈610 wppm.

3. NEUTRON IRRADIATION OF HYDRIDED SPECIMENS IN HFIR

During preparation of the hydride cladding specimens as discussed in Section 2, the hydrides are distributed uniformly within the cladding. This parameter is not prototypic of the hydride morphology generated under normal LWR operation. Under HFIR test irradiation conditions (at prototypic LWR cladding surface temperature and temperature gradient across the cladding wall), normal cladding end-state hydride morphology inside the cladding is expected within days of the start of irradiation. Two capsules (HYCD-1 and HYCD-2) were removed from the reactor after the first and third cycles of irradiation for post-irradiation examination (PIE) to determine the resulting end-state hydride morphology. The 6-in. cladding sample (HYCD-3) was included in the initial insertion to begin accumulating the required fast neutron fluence (which will require eight HFIR cycles). If the desired hydride morphology is confirmed from the PIE of HYCD-1 and HYCD-2, additional capsules containing 6-in. samples will be inserted in HFIR at later dates. The purpose of this section is to summarize the as-irradiated conditions (fluences and temperatures) for HYCD-1 and HYCD-2.

3.1 DESIGN DESCRIPTION

3.1.1 HFIR Target Facilities

HFIR is a beryllium-reflected, pressurized, light-water-cooled and moderated flux-trap-type reactor. The core consists of aluminum-clad involute-fuel plates, which currently utilizes highly enriched ^{235}U fuel at a power level of 85 MWt.

The reactor core, illustrated in Fig. 3.1, consists of two concentric annular regions, each approximately 61 cm in height. The flux trap is ~12.7 cm in diameter, and the outer fueled region is ~43.5 cm in diameter. The fuel region is surrounded by a beryllium annular reflector approximately 30.5 cm in thickness. The beryllium reflector is in turn backed up by a water reflector of effectively infinite thickness. In the axial direction, the reactor is reflected by water. The reactor core assembly is contained in a 2.44 m diameter pressure vessel, which is located in a 5.5 m cylindrical pool of water.

HYCD-1, HYCD-2, and HYCD-3 were placed in the flux trap of HFIR in positions E3, E6 and C2 respectively, as shown in Fig. 3.2. The fast neutron flux in these positions in HFIR is illustrated in Fig. 3.3 (as a function of core height).

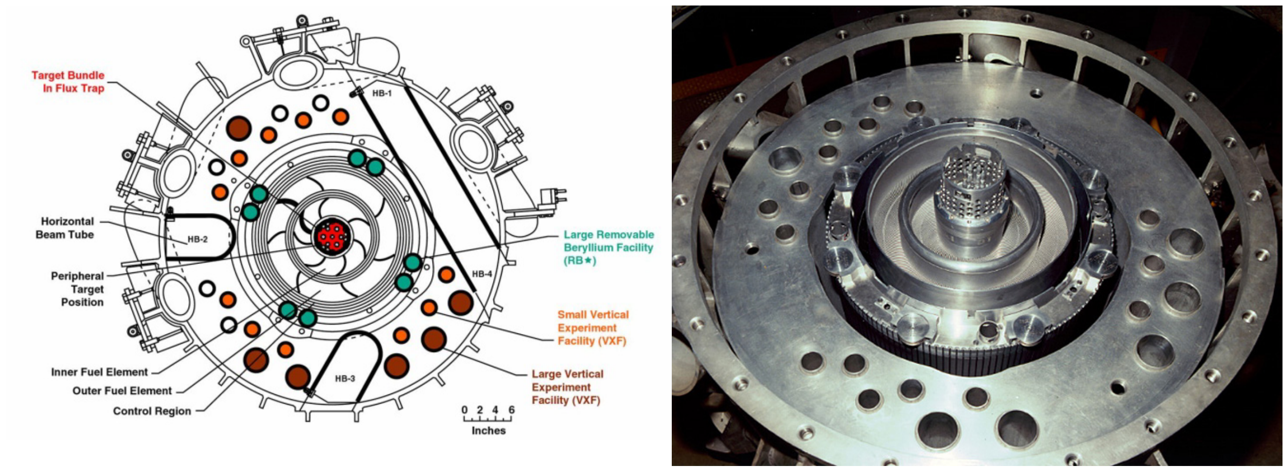

Fig. 3.1. Cross section through HFIR illustrating the primary experimental sites (left) and a picture of the reactor core (right).

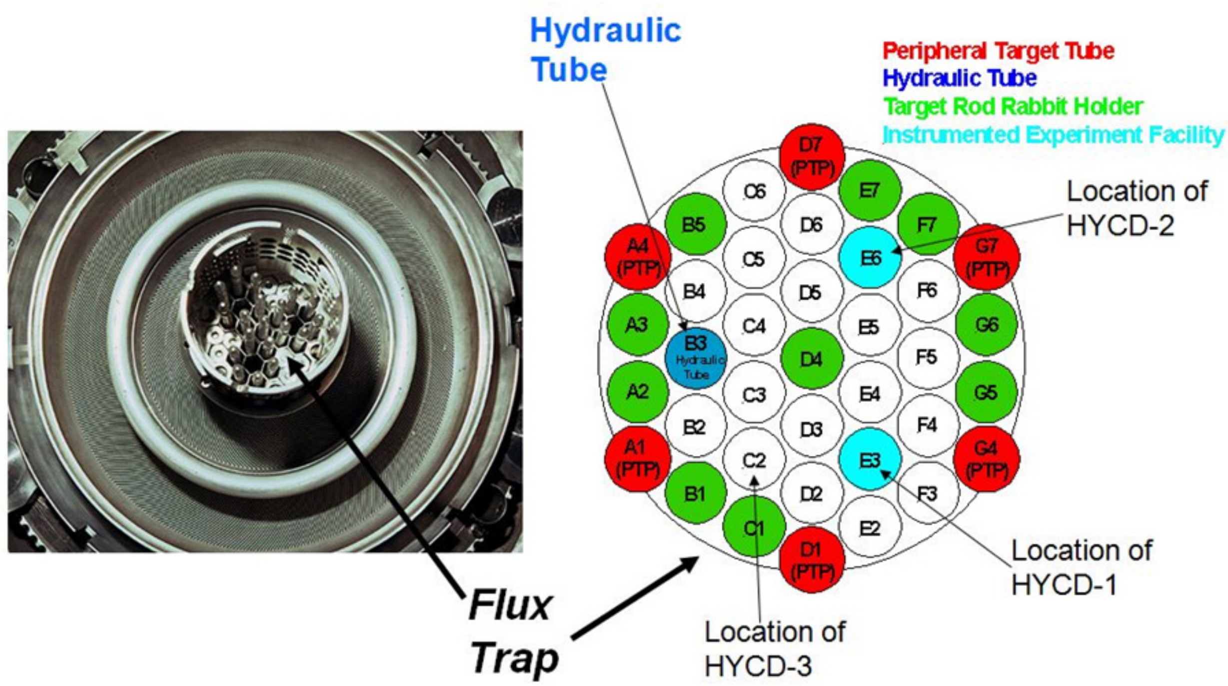

Fig. 3.2. Flux trap irradiation locations for HYCD-1, HYCD-2 and HYCD-3.

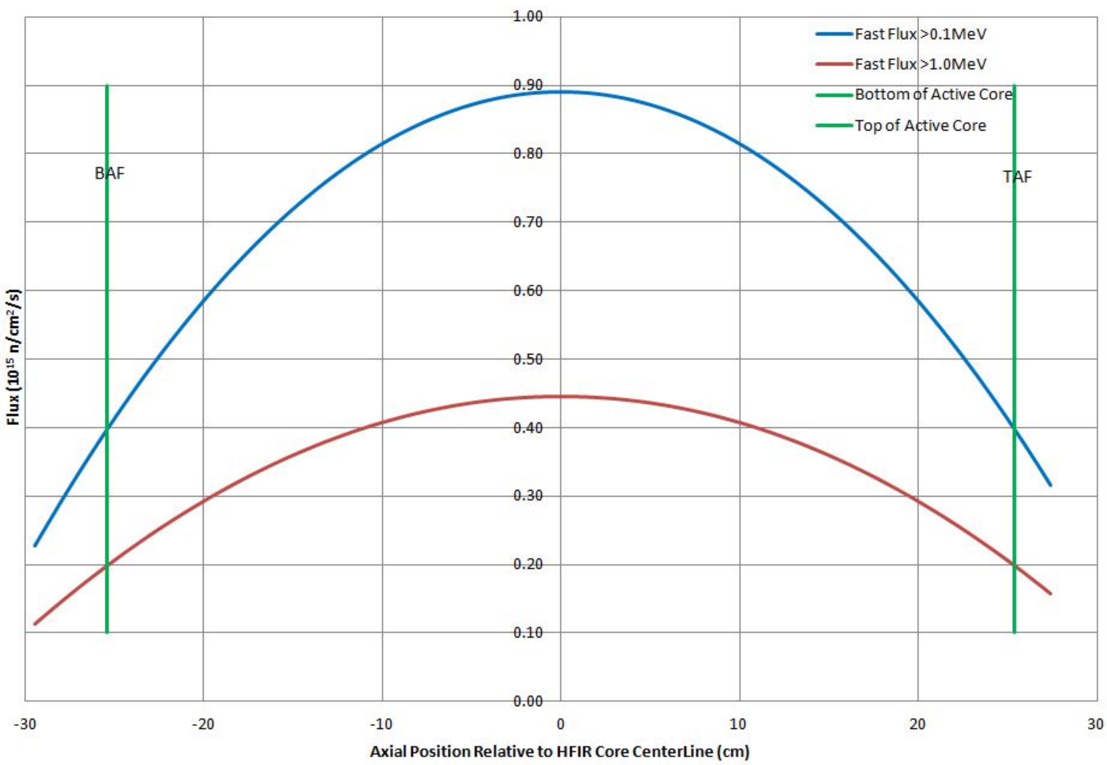

Fig. 3.3. HFIR fast neutron flux in the E3, E6 and C2 flux trap positions.

3.1.2 General Experiment Design Description

The experiment assembly is provided on Drawing X3E020977A608 (see Appendix C). A schematic of the assembly around the test specimens is illustrated in Fig. 3.4.

Coolant is directed to the experiment by the Al-6061 outer shroud. The outer aluminum housing is the primary containment for the experiment and is also fabricated from Al-6061. The housing is made from No. 17, ½-in. Al-6061 tubing, which has an inner diameter of 9.73 mm (0.383 in.). The ends of the tubing are bored out to an inner diameter of 11.3 mm (0.445 in.) to meet the requirements of the existing design for the top and bottom caps and the approved weld procedures.

The Zircaloy-4 clad specimens have an outer diameter of 9.5 mm (0.3741 in.) and an inner diameter of 8.35 mm (0.3287 in.). The clad length will range from 76 mm (3.00 in.) to 152 mm (6.00 in.). The clad is fitted with a molybdenum rod which acts as a heater for the cladding. The molybdenum rod is 102 mm (4 in.) long for the 76 mm clad case and 178 mm (7 in.) long for the 152 mm clad case. The axial location of the clad centroid is located at the reactor mid-plane. Spacers made from ⅜ in Al-6061 tubing are used to ensure this placement. For the 76 mm clad case, the top and bottom spacers are 224 mm (8.82 in.) and 227 mm (8.95 in.) respectively. Similarly, for the 152 mm clad case, the top and bottom spacers are 183 mm (7.22 in.) and 189 mm (7.45 in.) respectively. Both spacer sets are counterbored 12 mm (0.5 in.) at the end oriented closest to the reactor centerline to hold the excess molybdenum heater rod while also keeping the clad in the proper location. Six equi-spaced pads are punched into the ends of each spacer closest to the reactor center line. This feature produces a slightly larger diameter from the original outer diameter of the spacer tube, and this dimension is set to keep the experiment centered in the housing tube.

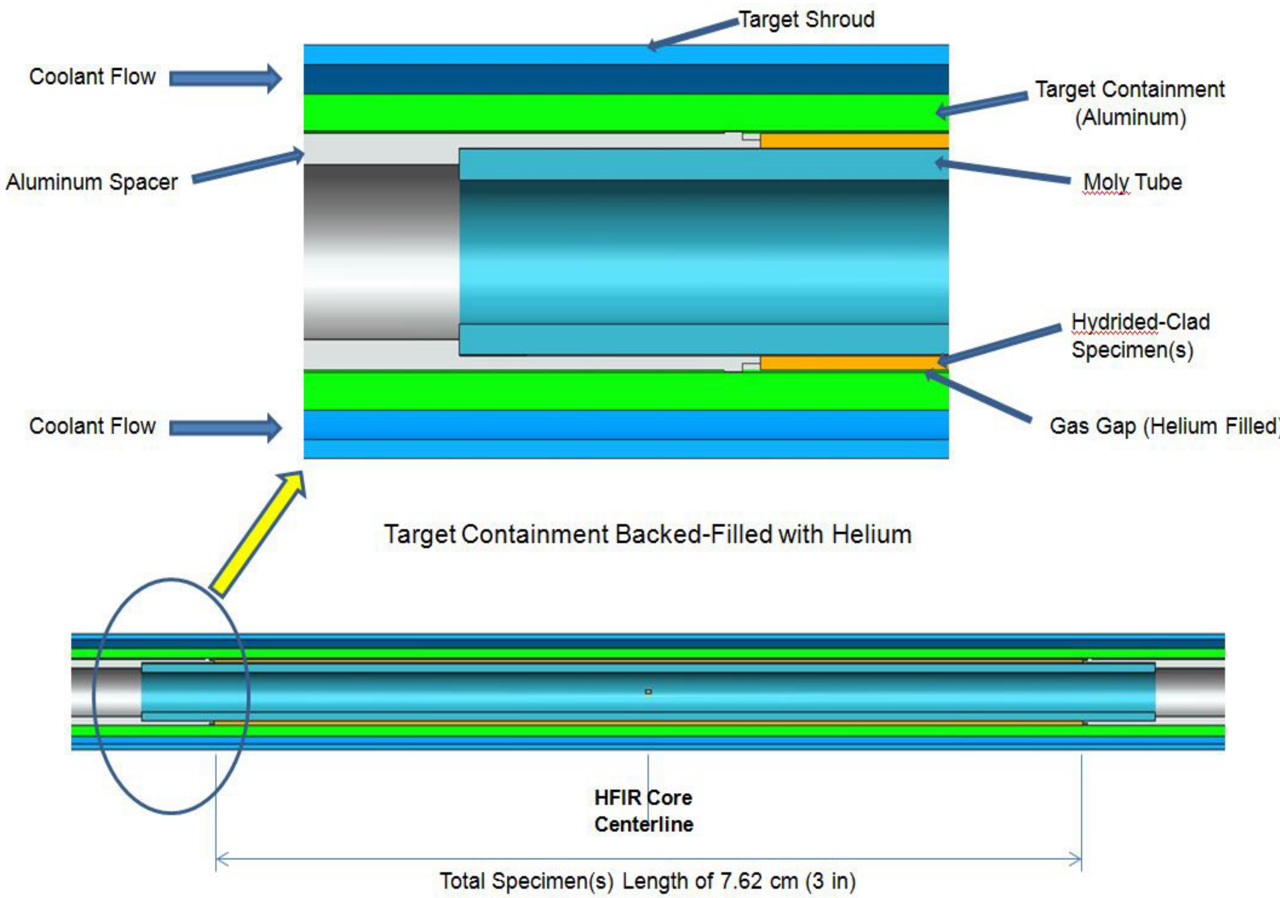

Fig. 3.4. Experiment assembly schematic.

3.1.3 HYCD-1 Assembly Description

The clad specimens (three samples, each 1 in. [2.54 cm] in length) utilized in HYCD-1 are given in Table 3.1. The location of these specimens within the experiment assembly is shown in Fig. 3.5.

Table 3.1. HYCD-1 clad specimens[1]

Specimen ID	Hydrogen content (wppm)
LRR4A20	<20
LRR1B5	~820
UCF1D1C	~450

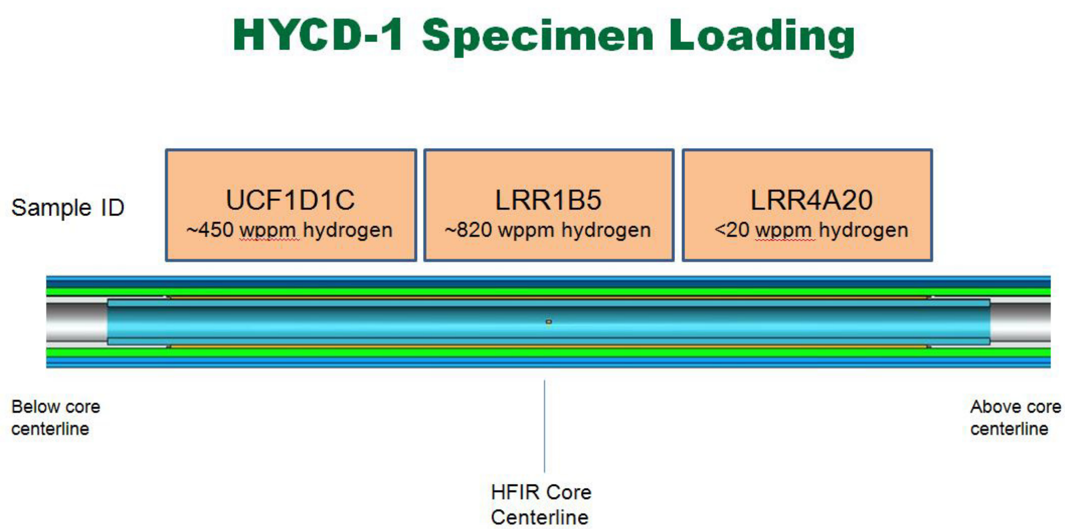

Fig. 3.5. HYCD-1 specimen loading.

3.1.4 HYCD-2 Assembly Description

The clad specimens (three samples, each 1 in. [2.54 cm] in length) utilized in HYCD-2 are given in Table 3.2. The location of these specimens within the experiment assembly is shown in Fig. 3.6.

Table 3.2. HYCD-2 clad specimens

Specimen ID	Hydrogen content (wppm)
LRR4A23	<20
LRR1D7	~550
UCF1D1E	~450

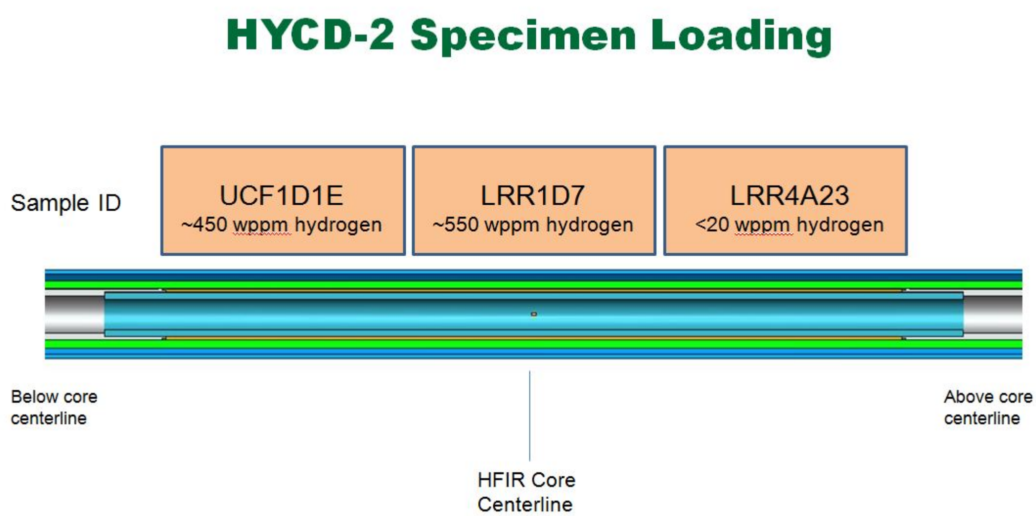

Fig. 3.6. HYCD-2 specimen loading.

3.2 HFIR OPERATING CONDITIONS DURING THE IRRADIATION OF HYCD-1 AND HYCD-2

3.2.1 HFIR Operating History

HYCD-1, HYCD-2 and HYCD-3 were inserted in HFIR for Cycle 440B; HYCD-1 was removed after Cycle 440B and HYCD-2 after Cycle 442. The HFIR operating history for these cycles is illustrated in Fig. 3.7.

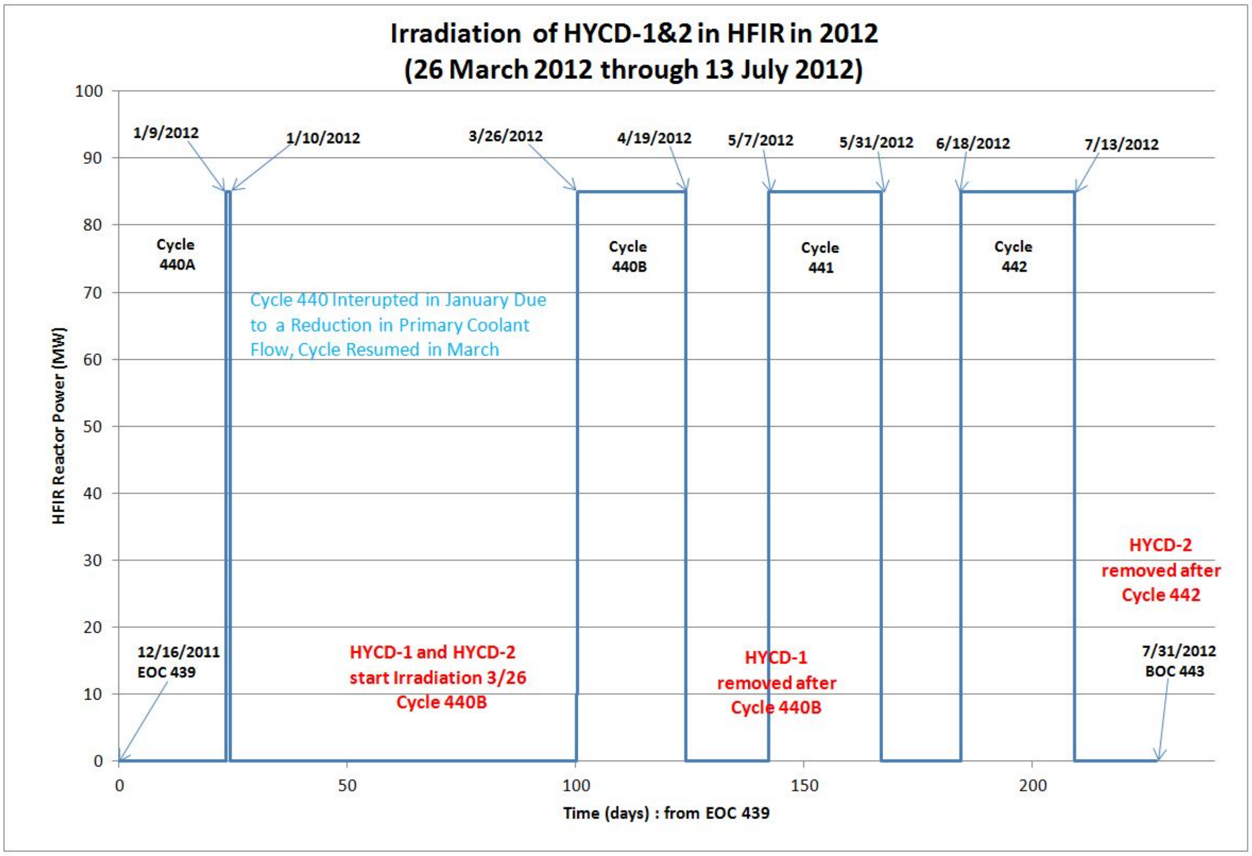

Fig. 3.7. HFIR operating history during the HYCD-1 and HYCD-2 irradiations.

The days of powered operation for Cycles 440B, 441 and 442 are given in Table 3.3 (from operator logs on power ascension and time of SCRAM).

Table 3.3. **HFIR powered operation for Cycles 440B, 441, and 442**

Cycle	Powered operation (days)
440B	23.84
441	24.66
442	24.90

3.2.2 HYCD-1 and HYCD-2 Accumulated Fast Fluence

Given the neutron flux at the E3 and E6 positions (illustrated in Fig. 3.3) and the periods of powered operation in HFIR (Table 3.3), it is a straightforward calculation to determine the fast (>1.0 MeV) neutron fluence attained by the HYCD-1 and HYCD-2 specimens. The fast fluence (>1.0 MeV) accumulated in the HYCD-1 specimens is shown in Fig. 3.8 and tabulated in Table 3.4.

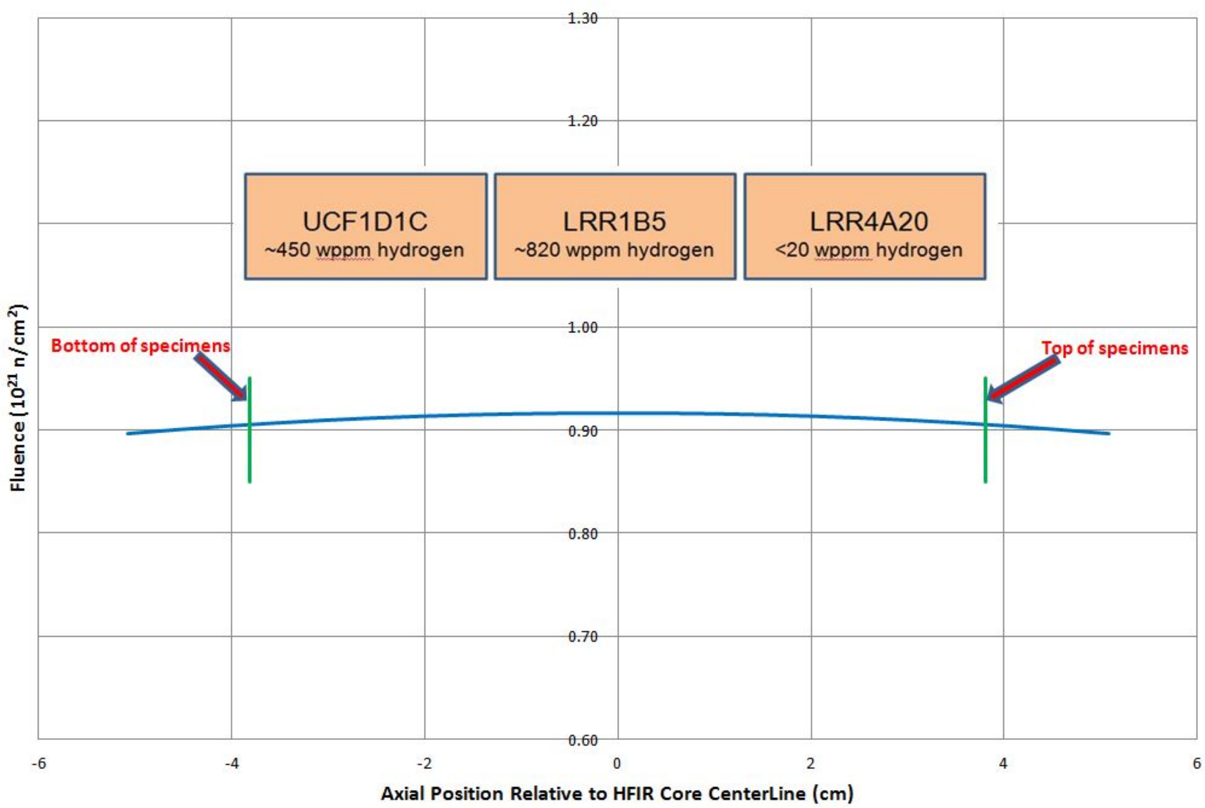

Fig. 3.8. Fast fluence (>1.0 MeV) in the HYCD-1 specimens.

Table 3.4. HYCD-1 clad specimen fast fluences (>1.0 MeV)

Specimen ID	Hydrogen content (neutrons/cm^2)
LRR4A20	0.911e21 (±0.004)
LRR1B5	0.916e21 (±0.001)
UCF1D1C	0.911e21 (±0.004)

The fast fluence (>1.0 MeV) accumulated in the HYCD-2 specimens is shown in Fig. 3.9 and tabulated in Table 3.5.

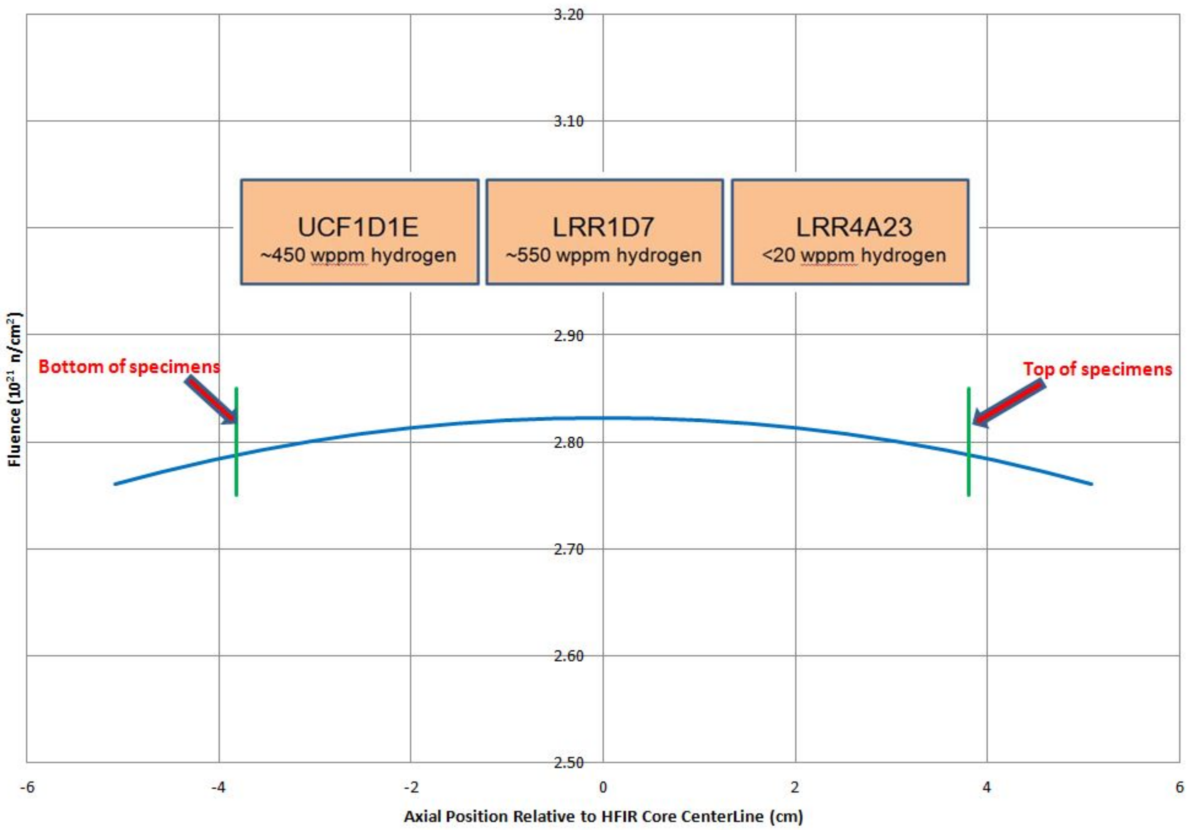

Fig. 3.9. Fast fluence (>1.0 MeV) in the HYCD-2 specimens.

Table 3.5. HYCD-2 clad specimen fast fluences (>1.0 MeV)

Specimen ID	Hydrogen content (neutrons/cm^2)
LRR4A23	2.805e21 (±0.013)
LRR1D7	2.820e21 (±0.002)
UCF1D1E	2.805e21 (±0.013)

3.2.3 HYCD-1 and HYCD-2 Operating Temperatures

Since these capsules were not instrumented, the operating temperatures within the capsules are based on best-estimate simulations (design analysis and calculation [DAC], DAC-11-19-HYDRIDE01, February 2012, performed by R. Howard). A description of the ANSYS model and supporting DACs (fluid boundary conditions, component heat generation rates, materials of construction, finite element model, etc.) are given in DAC-11-19-HYDRIDE01. These simulations provided the "best-estimate" operating inner and outer surface temperatures of the HYCD-1 and HYCD-2 specimens shown in Fig. 3.10. The radial temperature drop across the specimen(s) is illustrated in Fig. 3.11. The temperatures and temperature drops experienced (calculated) for each of the specimens in HYCD-1 and HYCD-2 are tabulated in Table 3.6.

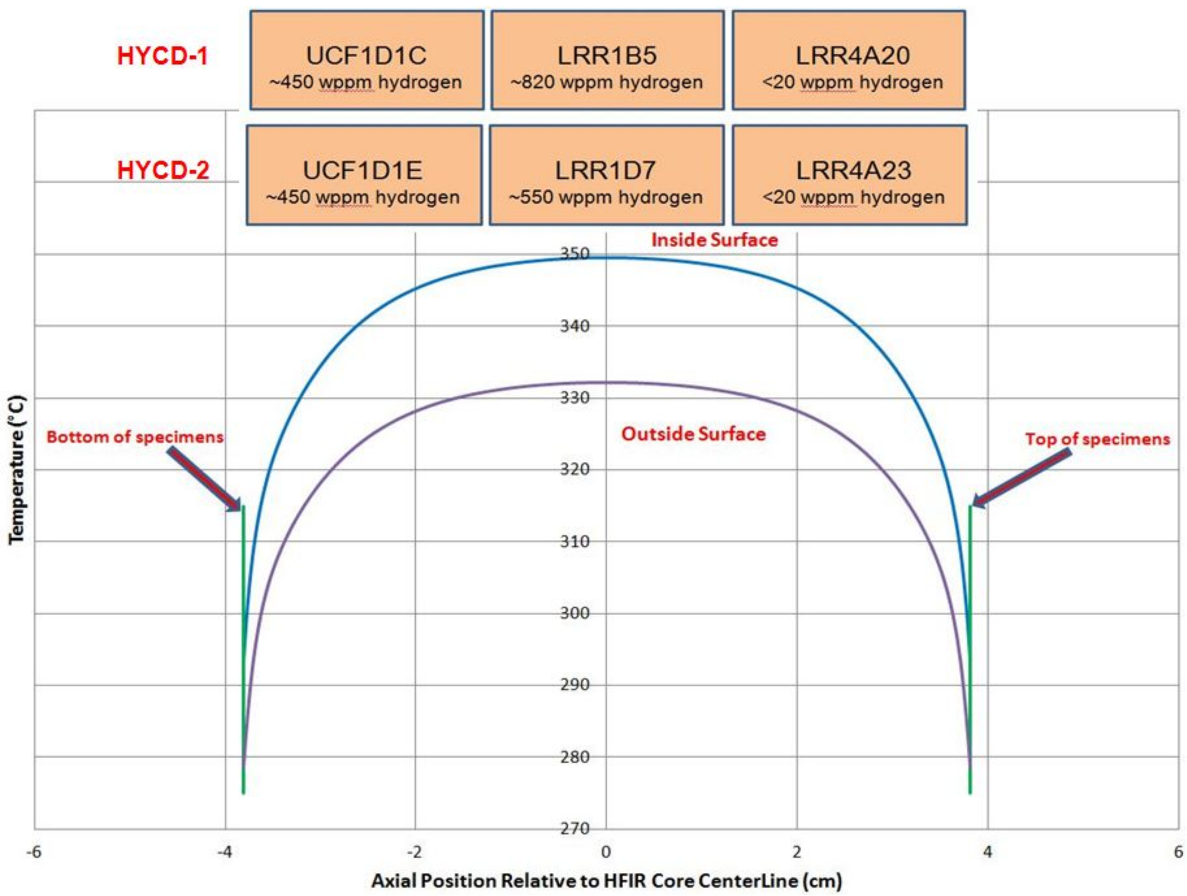

Fig. 3.10. HFIR operating temperatures in the HYCD-1 and HYCD-2 specimens.

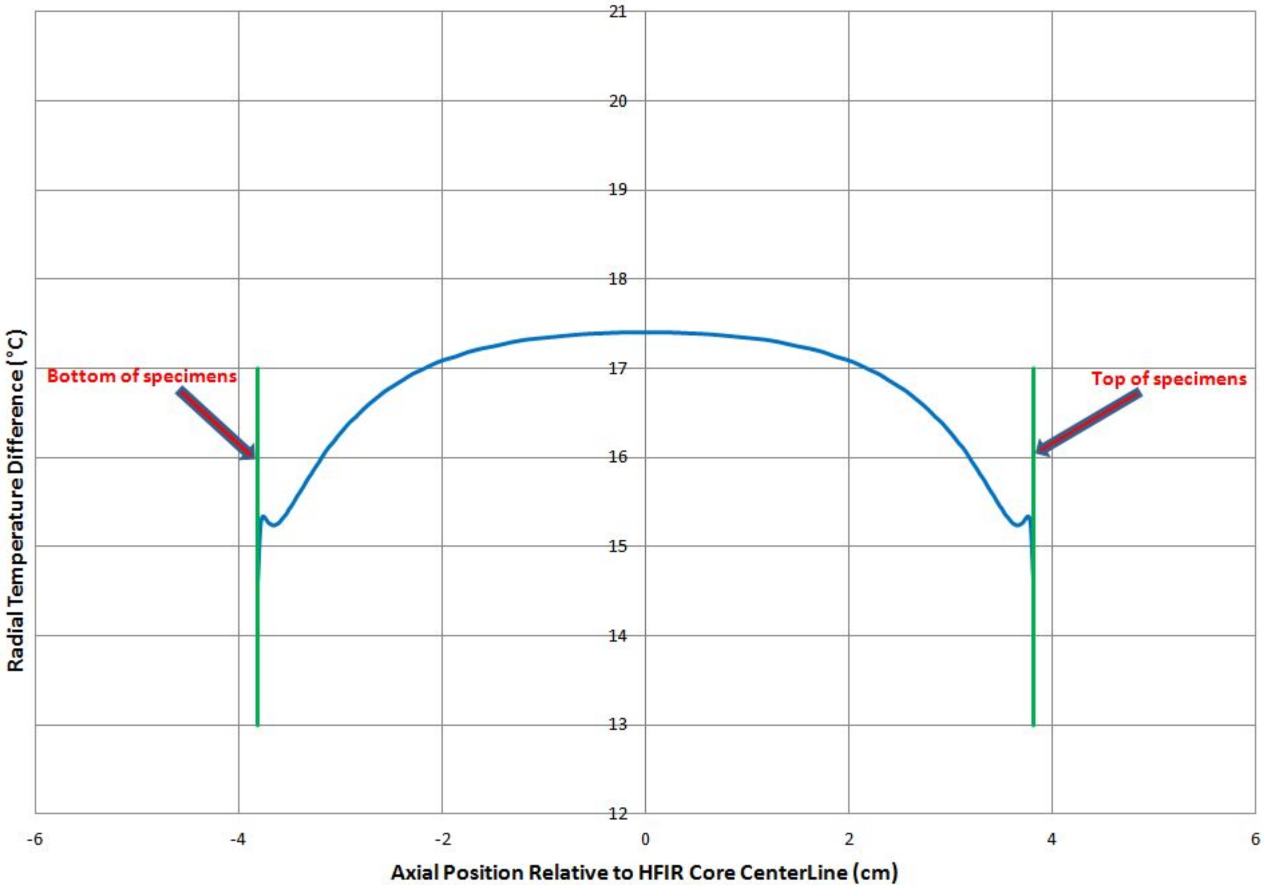

Fig. 3.11. Operating radial temperature drop in the HYCD-1 and HYCD-2 specimens.

Table 3.6. Operating temperatures in the HYCD-1 and HYCD-2 clad specimen(s)

Position [cm] (relative to core centerline)	-3.81 to -1.27	-1.27 to +1.27	+1.27 to +3.81
HYCD-1			
Specimen ID	UCF1D1C	LRR1B5	LRR4A20
Avg. inner surface temperature (°C)	324.92	348.94	324.92
Inner surface temp. range (°C)	293.2 to 348.1	348.1 to 349.5	293.2 to 348.1
Avg. outer surface temperature (°C)	308.97	331.57	308.97
Outer surface temp. range (°C)	278.6 to 330.8	330.8 to 332.1	278.6 to 330.8
Avg. temperature drop across specimen (°C)	15.95	17.37	15.95
ΔT Range (°C)	14.60 to 17.31	17.31 to 17.41	14.60 to 17.31
HYCD-2			
Specimen ID	UCF1D1E	LRR1D7	LRR4A23
Avg. inner surface temperature (°C)	324.92	348.94	324.92
Inner surf. temp. range (°C)	293.2 to 348.1	348.1 to 349.5	293.2 to 348.1
Avg. outer surface temperature (°C)	308.97	331.57	308.97
Outer surf. temp. range (°C)	278.6 to 330.8	330.8 to 332.1	278.6 to 330.8
Avg. temperature drop across specimen (°C)	15.95	17.37	15.95
ΔT Range (°C)	14.60 to 17.31	17.31 to 17.41	14.60 to 17.31

There are significant axial temperature gradients in the top and bottom 1 in. (2.54 cm) clad specimens in both HYCD-1 and HYCD-2 (there is very low variation in the middle specimen). There are three primary reasons for these axial temperature gradients: (1) the structural gamma heating is at its maximum at the core centerline and decreases with increasing distance from the core centerline; (2) the structural gamma heating is greater for molybdenum (~43.3 W/g [centerline]) than the Zircaloy clad specimen (~38.5 W/g) and the aluminum spacers (~32.5 W/g); and (3) the thermal conductivity of aluminum is greater than that of the molybdenum and Zircaloy. Thus, not only does the total power generated decrease (away from the core centerline) but heat is also being conducted axially from the molybdenum heater to the colder aluminum spacers. These axially temperature variations are most acute in the smaller 3 in. (7.62 cm) capsules (HYCD-1 and HYCD-2); there will be gradients in the larger 6 in. (15.24 cm) capsules (HYCD-3) but the variation seen here would be confined to the top and bottom ~2 cm of the cladding specimens.

4. PRELIMINARY PIE RESULTS OF IRRADIATED SPECIMENS HYCD-1 AND HYCD-2

4.1 VISUAL EXAMINATION OF HYCD-1 AND HYCD-2

After removal from the reactor, the HYCD-1 and HYCD-2 capsules were shipped to the Irradiated Fuel Examination Lab (IFEL) with a loop cask (see Fig. 4.1) for PIE. The cask arrived at the IFEL from the HFIR on November 6, 2012, approximately four months after HYCD-2 was removed from the reactor core. The two capsules were removed from the shipping cask and loaded into the hot cell in January 2013 (see Fig. 4.2 and Fig. 4.3). They were identified by the labeling engraved on the capsule shroud tube as HYCD-1 and HYCD-2. The capsules appeared to be in good condition and no unusual features were noted.

Hydrided specimens were removed from the capsules by milling out the shroud and aluminum target containment at a location 4 in. from the marked feature towards the capsule centerline (see Fig. 4.4), removing the aluminum spacers, and pushing out the cladding specimen from the molybdenum heater rod (see Fig. 4.5 and Fig. 4.6). The HYCD-1 specimens were removed rather easily. The HYCD-2 case proved to be a more difficult matter and a great deal of force was needed to remove cladding specimens UFC1D1E and LRR1D7 from the molybdenum heater rod. It should be noted that these cladding specimens may have been damaged during this process. Figures 4.7 and 4.8 show the specimens after they were removed from HYCD-1 and HYCD-2 respectively. Figure 4.9 is a high magnification image of Specimen UCF1D1E, which shows some unusual feature near the middle of cladding sample.

Fig. 4.1. Loop cask for HYCD-1 and HYCD-2 (OD × L = 2 ft × 8 ft), at the IFEL.

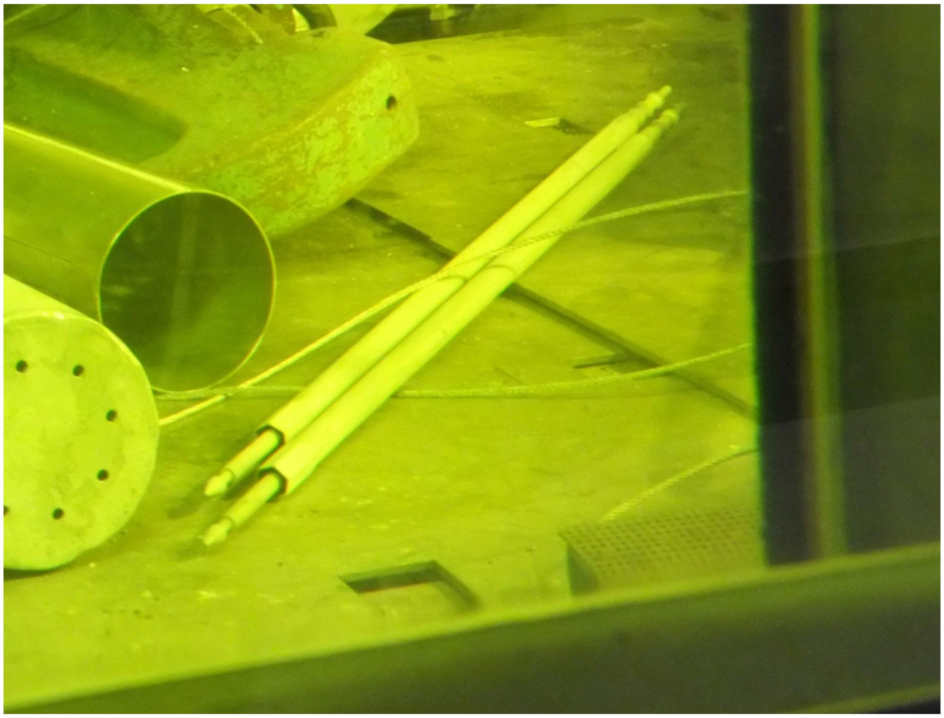

Fig. 4.2. HYCD-1 and HYCD-2 capsules in the North Cell of 3525.

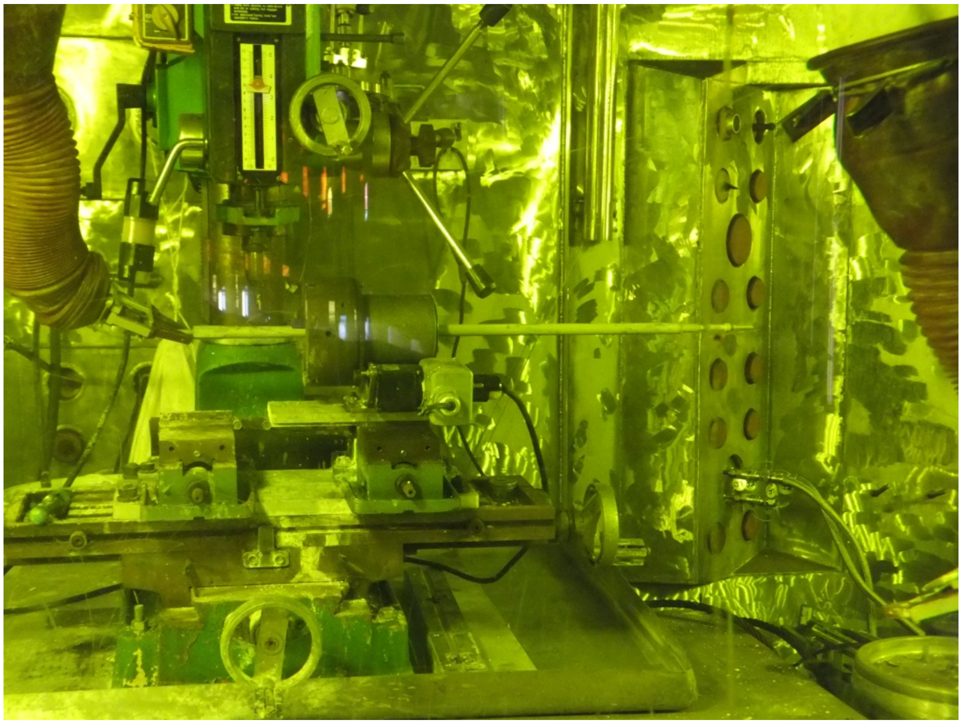

Fig. 4.3. In-cell milling to remove the cladding specimen from the capsule.

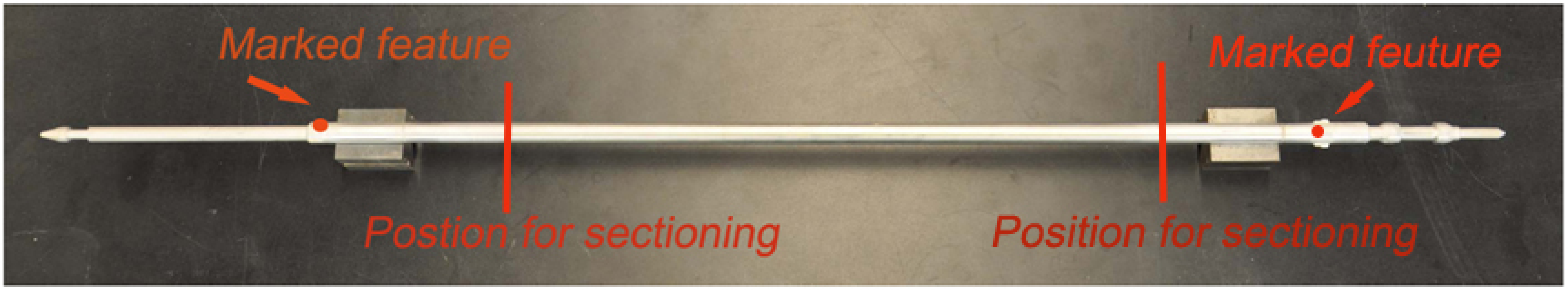

Target Capsule without shroud

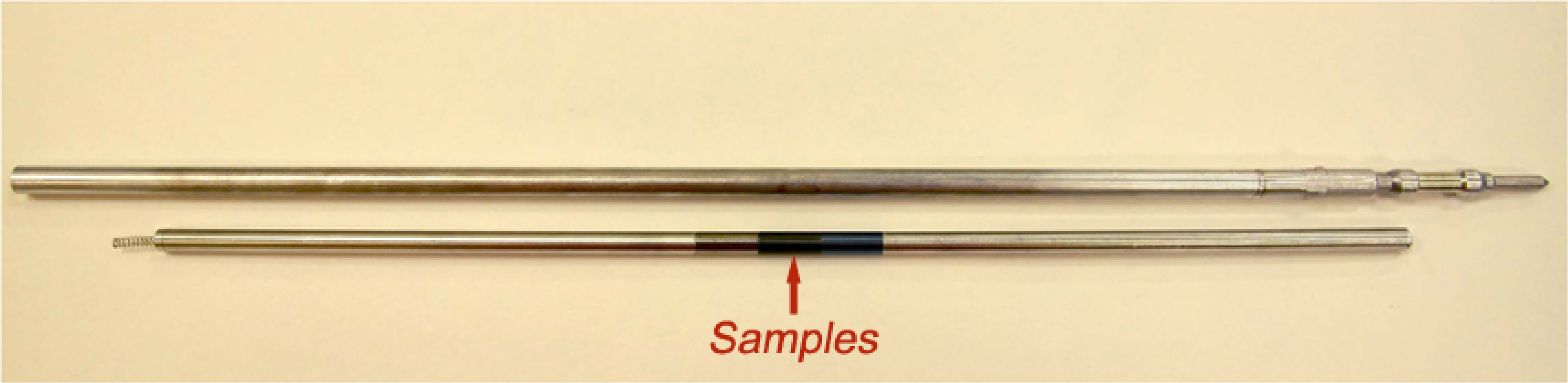

Target Capsule (without top cap) and internal components (3 in sample)

Fig. 4.4. Illustration of removing the cladding specimens from the capsule.

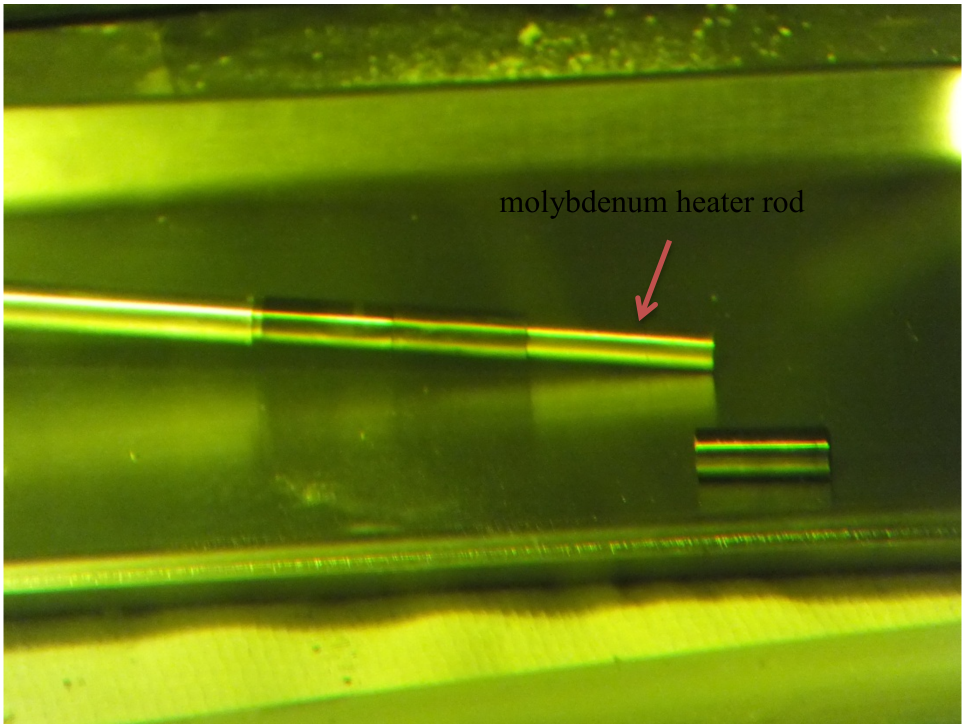

Fig. 4.5. HYCD-1 samples on molybdenum heater rod.

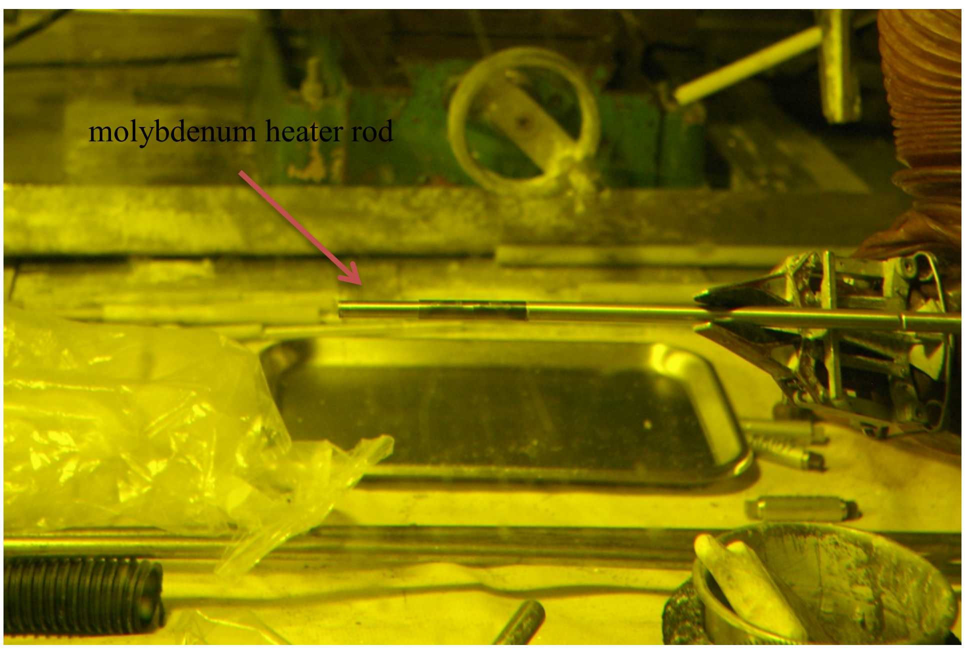

Fig. 4.6. HYCD-2 samples on molybdenum heater rod.

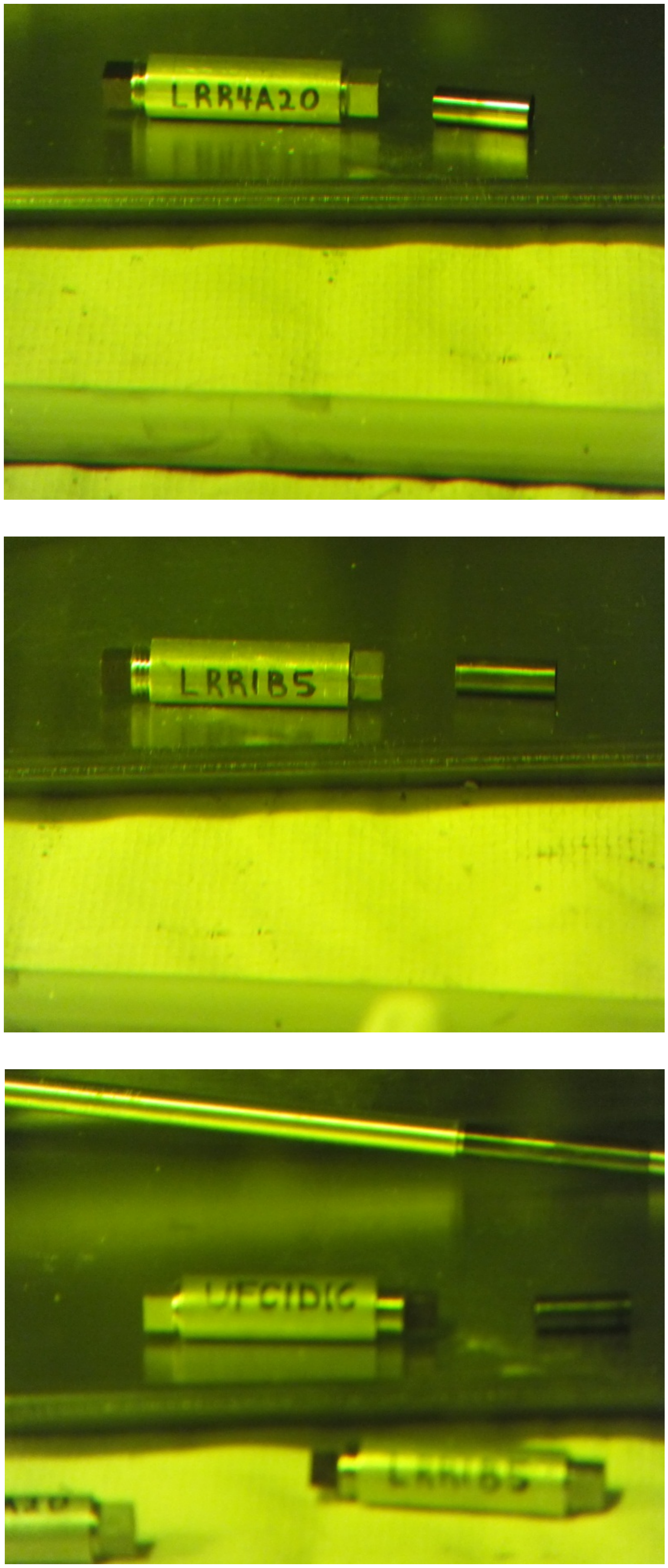

Fig. 4.7. Specimens removed from HYCD-1.

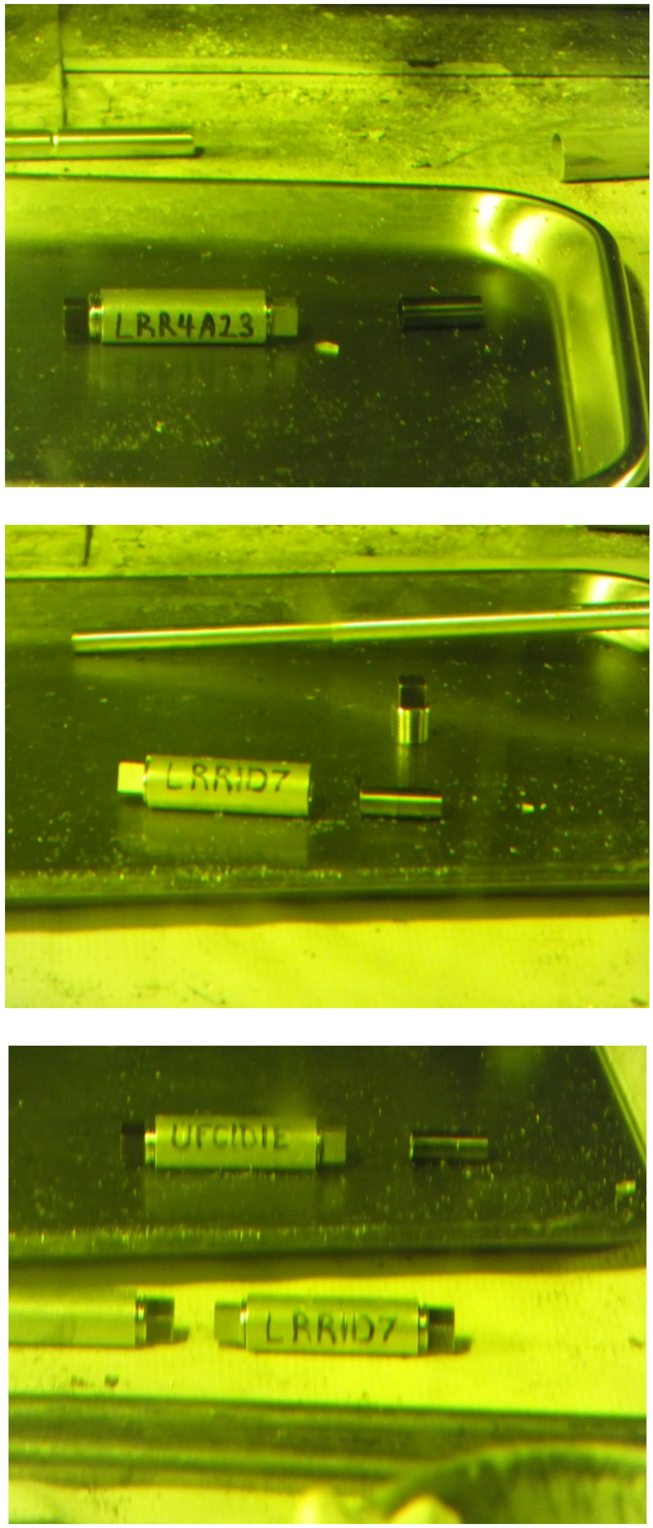

Fig. 4.8. Specimens removed from HYCD-2.

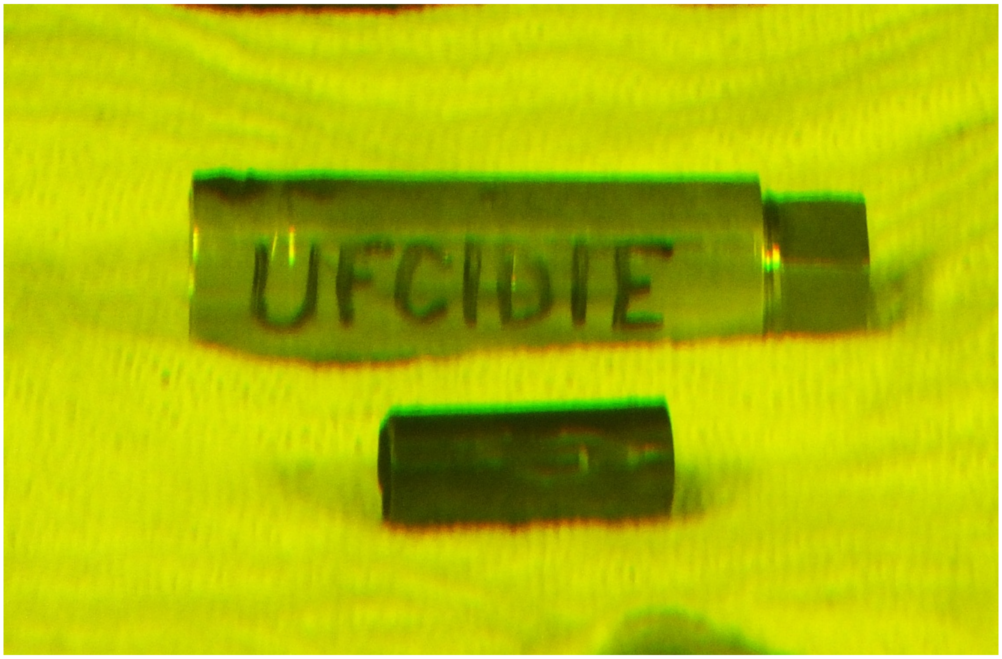

Fig. 4.9. High magnification image of Specimen UFC1D1E.

4.2 DOSE RATE MEASUREMENTS

Dose rates of the HYCD-1 and HYCD-2 specimens were measured at 1 in. and 12 in., as illustrated in Fig. 4.10. The detector used for the measurement is a Thmers Eberline RO20 Ion Chamber. For each capsule, one 1-in.-long specimen was selected. Table 4.1 summarized the measured dose rates. An ORNL Radiological Survey report in support of dose rating for these two HYCD-1 and HYCD-2 specimens is attached in Appendix A.

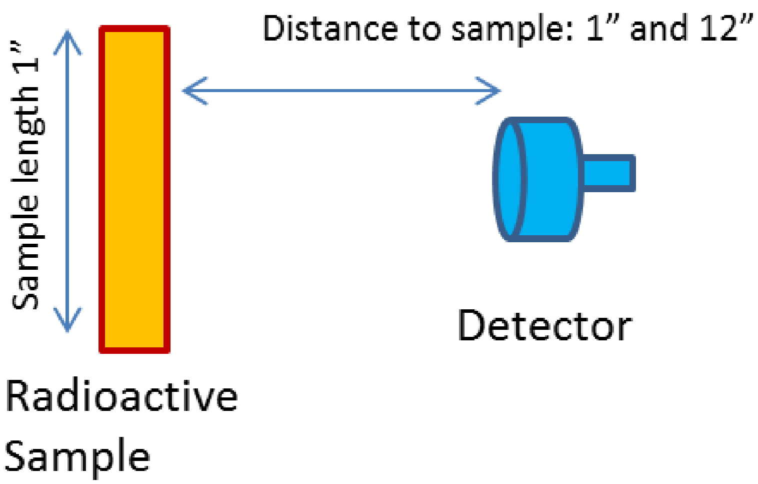

Fig. 4.10. Schematic illustration of the dose rate measurement on HYCD-1 and HYCD-2.

Table 4.1. Dose rates on the HYCD-1 and HYCD-2 specimens

Capsule ID	HYCD-1	HYCD-2
Sample ID	UFC1D1C	LRR1D7
Cycle(s) in HFIR	1	3
Sample length	25.4 mm	25.4 mm
Wall thickness	0.57 mm	0.57 mm
Materials	Zircaloy-4	Zircaloy-4
Hydrogen content	≈450 wppm	≈550 wppm
Date removed from reactor	4/19/2012 - 5/7/2012	7/13/2012 – 7/31/2012
Date measured	2/18/2013	2/18/2013
Dose rate[a] at 1 cm	20 R/h	40 R/h
Dose rate[a] at 30 cm	1 R/h	4 R/h
Comments	---	---

[a]Background dose rate in the work ranged from 35 mR/h.

4.3 OPTICAL METALLOGRAPHIC EXAMINATION

Sample UFC1D1C was selected from HYCD-1 capsule and LRR1D7 from HYCD-2 for microstructural examinations. Both samples are 1 in. long, which were sectioned by a diamond saw (see Fig. 4.11) in hot cell into five shorter rings, as shown in Figs. 4.12 and 4.13. Two optical metallographic mounts, as listed in Table 4.2, were prepared by mounting the cut specimens (the middle rings shown in Figs. 4.12 and 4.13) with epoxy in a phenolic base mount. These mounts were then ground flat and polished. After a final cleaning they were photographed using a commercial metallographic microscope and the images were assembled into a final collage (see Figs. 4.14 and 4.15). No unusual behavior was noted for Sample 6376. However, two through-wall cracks were observed for Sample 6377 (see Fig. 4.16). As the MET mount were prepared using the same process for the both samples, it is unlikely the cracks were introduced during the sample preparation. It appears that the damage was caused by sample removing from the HYCD-2 molybdenum heater rod. A design change for the capsule is under consideration to avoid such a problem in the future.

Optical microscopy with as-polished MET mounts samples did not clearly indicate the hydride morphology. Metallographic examinations of the etched samples are under way, and will be reported in the near future.

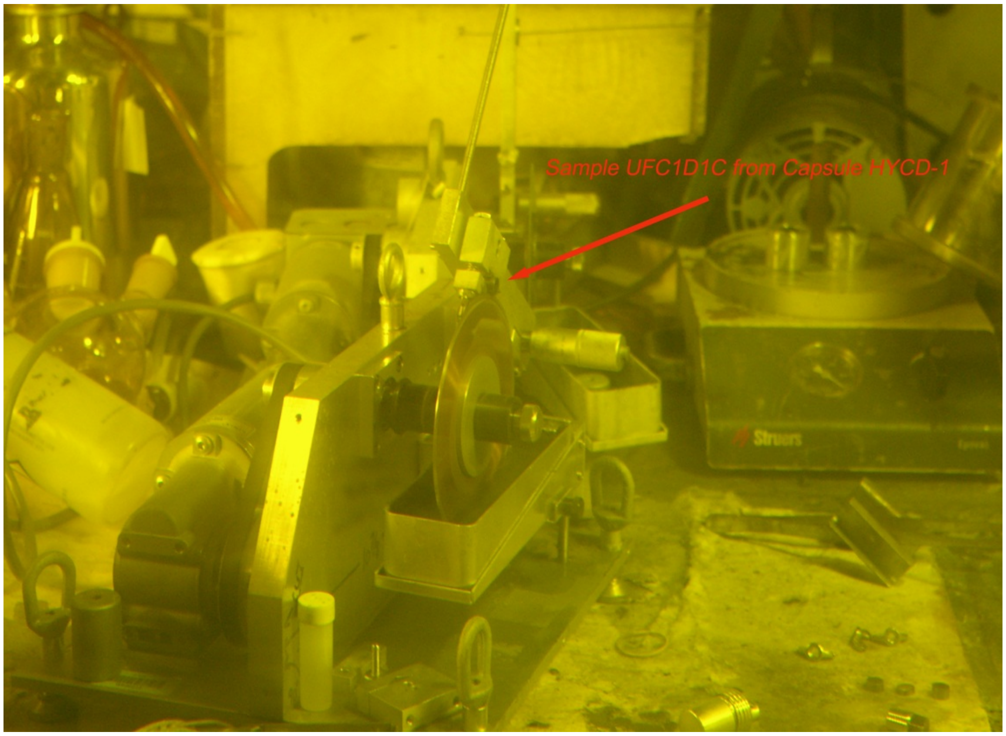

Fig. 4.11. A diamond saw for radioactive sample sectioning in hot cell.

Table 4.2. Summary of the MET mounts for optical metallographic examination

MET mount ID	6376	6377
Capsule ID	HYCD-1	HYCD-2
Sample sectioned	UFC1D1C	LRR1D7
Cycle(s) in HFIR	1	3
Wall thickness	0.57 mm	0.57 mm
Materials	Zircaloy-4	Zircaloy-4
Hydrogen content	≈450 wppm	≈550 wppm
Comments		2 cracks observed

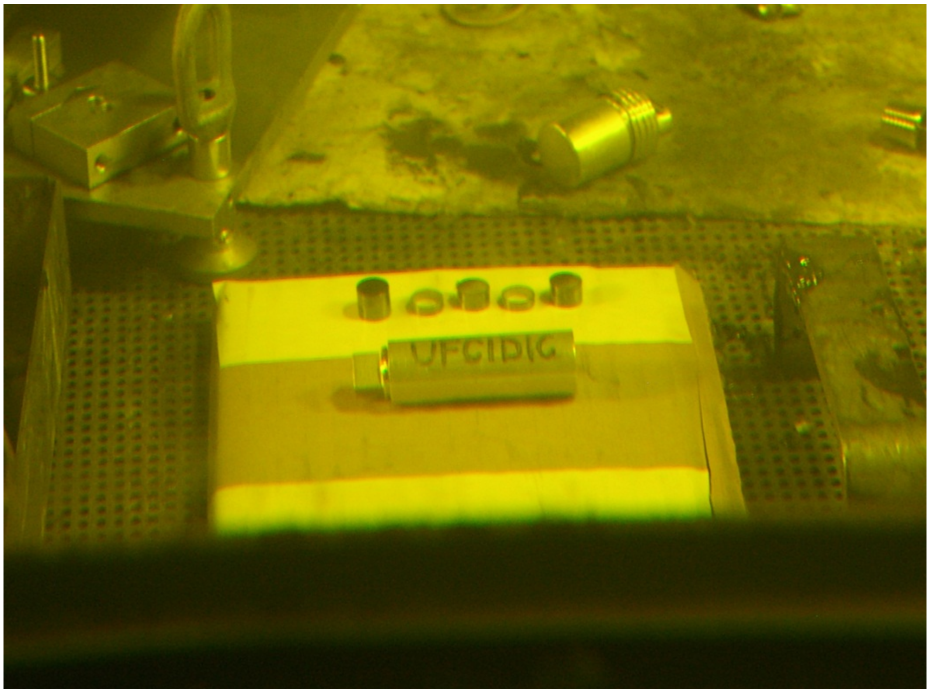

Fig. 4.12. Five rings sectioned from Sample UFC1D1C, Capsule HYCD-1.

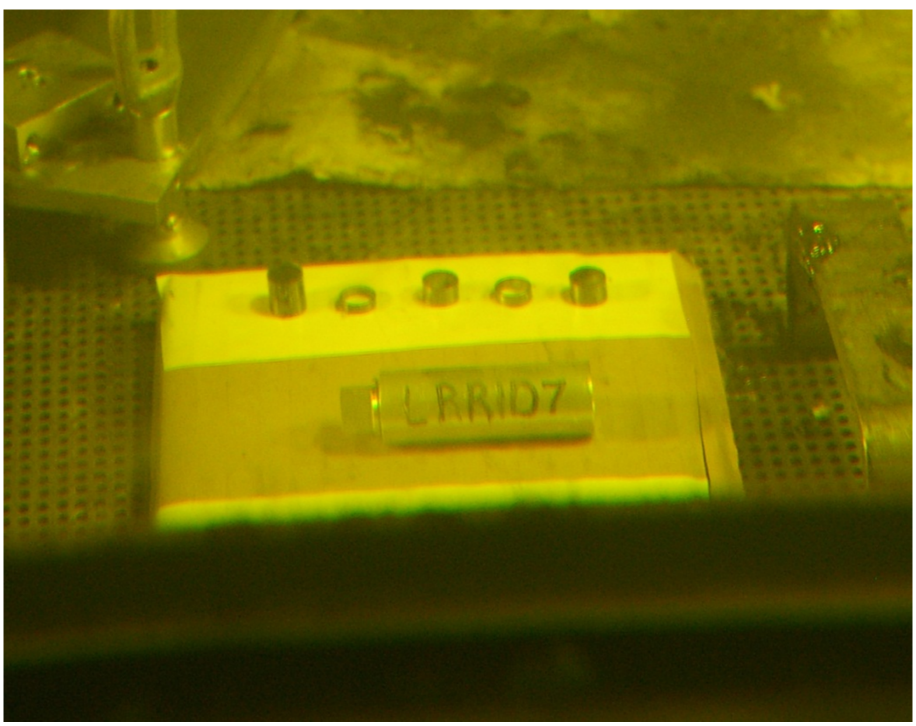

Fig. 4.13. Five rings sectioned from Sample LRR1D7, Capsule HYCD-2.

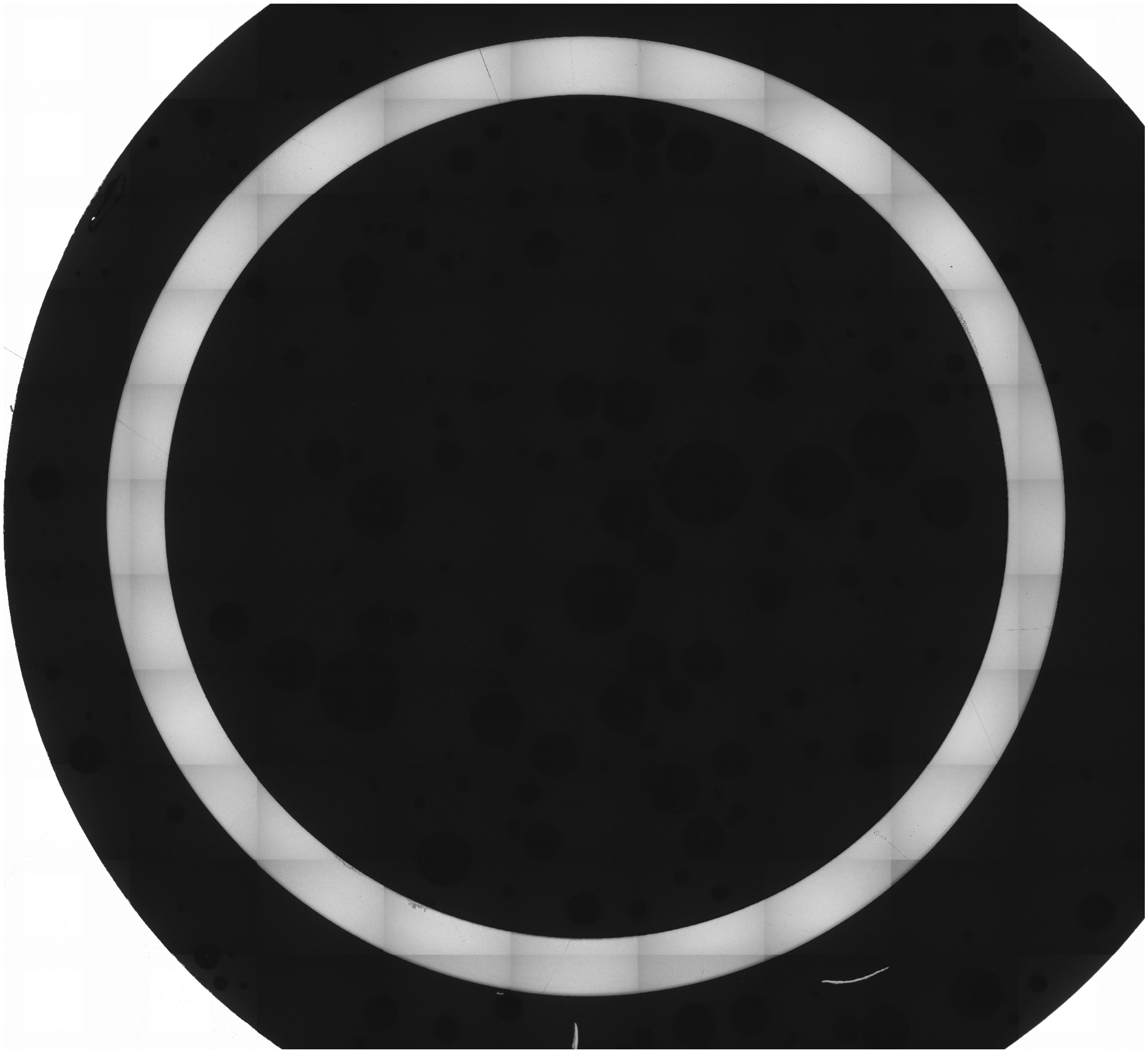

Fig. 4.14. Mount 6376, prepared from Sample UFC1D1C of Capsule HYCD-1. No unusual behavior was noted.

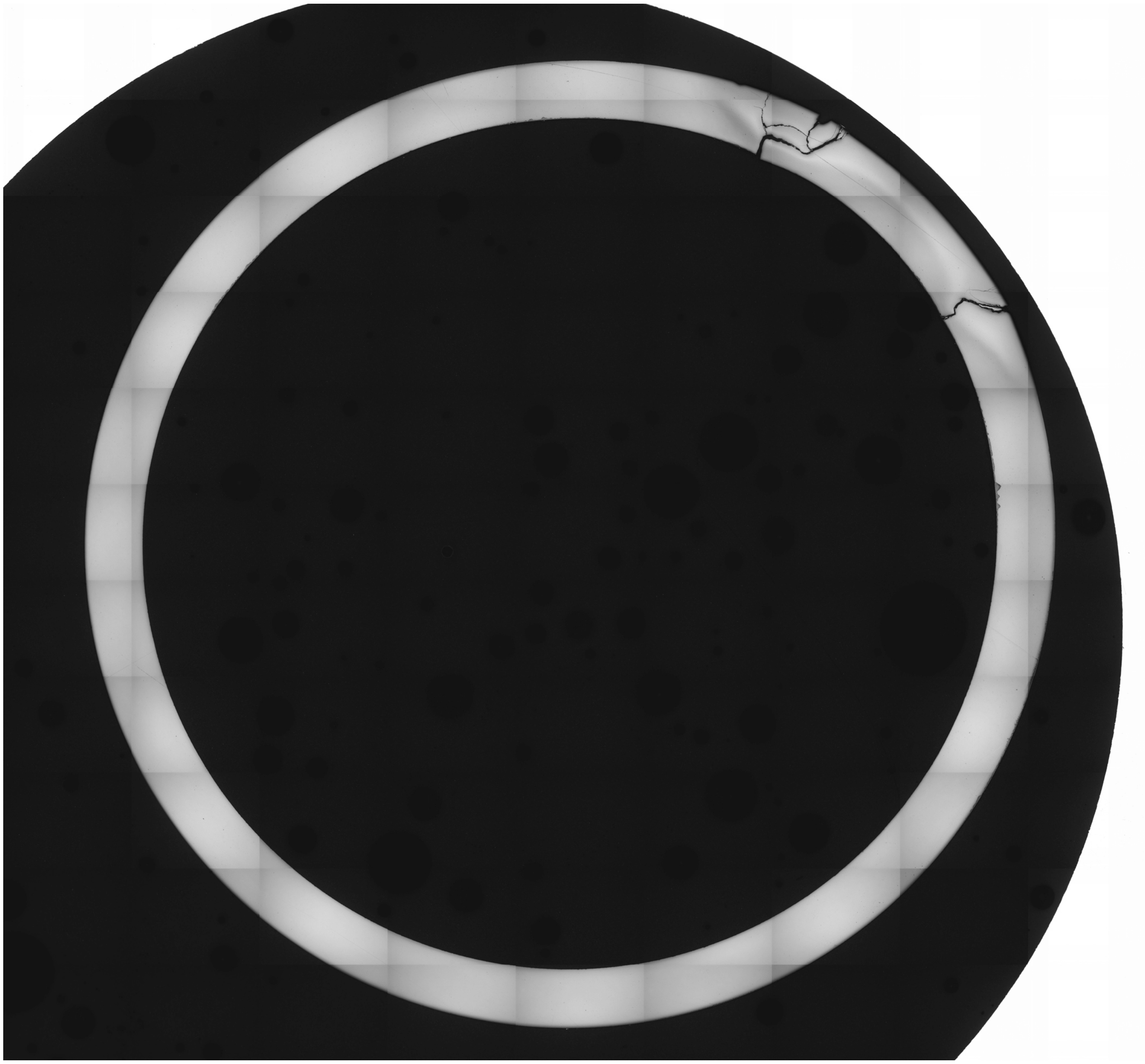

Fig. 4.15. Mount 6377, prepared from Sample LRR1D7 of Capsule HYCD-2. Two through wall cracks was observed.

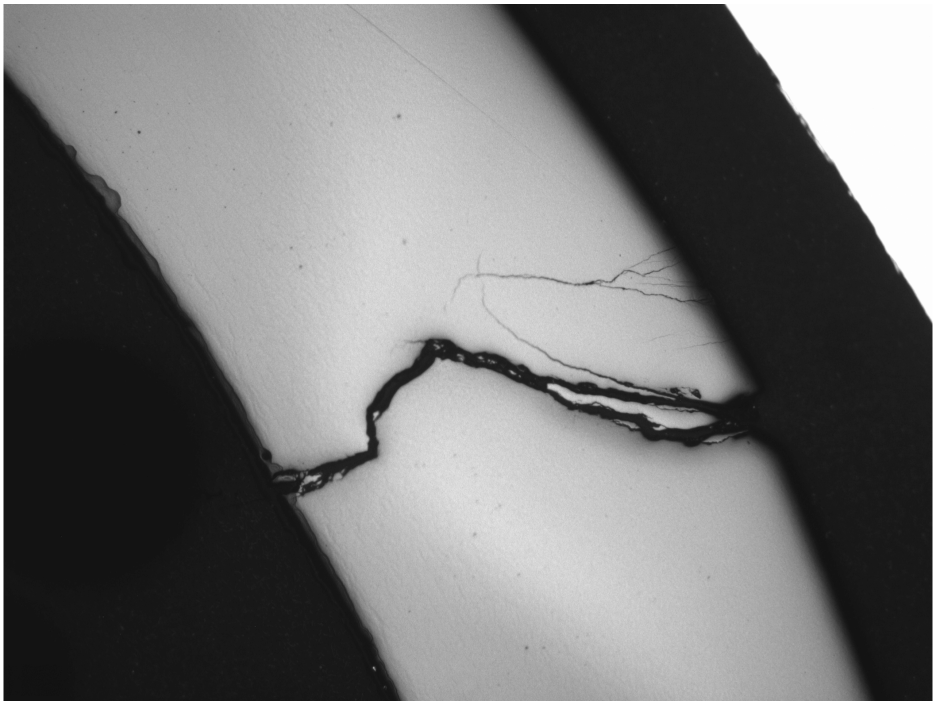

(a)

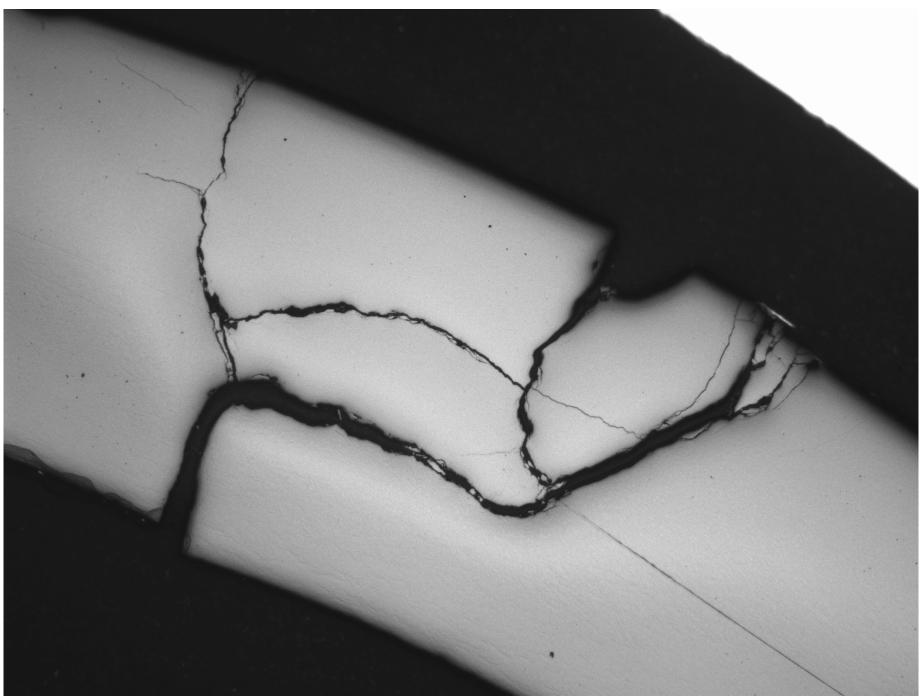

(b)

Fig. 4.16. High magnification images of the two cracks observed in Fig. 4.15.

4.4 OUTER DIAMETER MEASUREMENTS

Outer diameter (OD) measurements were conducted with a measurement sensor (Fig. 4.17), remotely operated in main hot cell in the IFEL for Specimens LRR4A20 & LRR1B5 from HYCD-1 and Specimens LRR4A24 & UFC1D1E from HYCD-2. Prior to the beginning of the measurement, the system was verified with a pin gauge standards, nominally 0.2450 in. (Fig. 4.18). As shown in Fig. 4.19, the measure sensor can record the OD value up to 0.00001 in.

The measurement indicates that the OD of the hydrided samples (LRR1B5 from HYCD1 and UFC1D1E from HYCD-2) is slightly increased, compared to the nominal OD of the unirradiated sample (Table 4.3). However the OD of the as-fabricated samples (LRR4A20 from HYCD-1 and LRR4A23 from HYCD-2) almost remains the same as the unirradiated samples. Tables 4.4 and 4.5 summarize the measured OD results for HYCD-1 and HYCD-2 specimens, respectively.

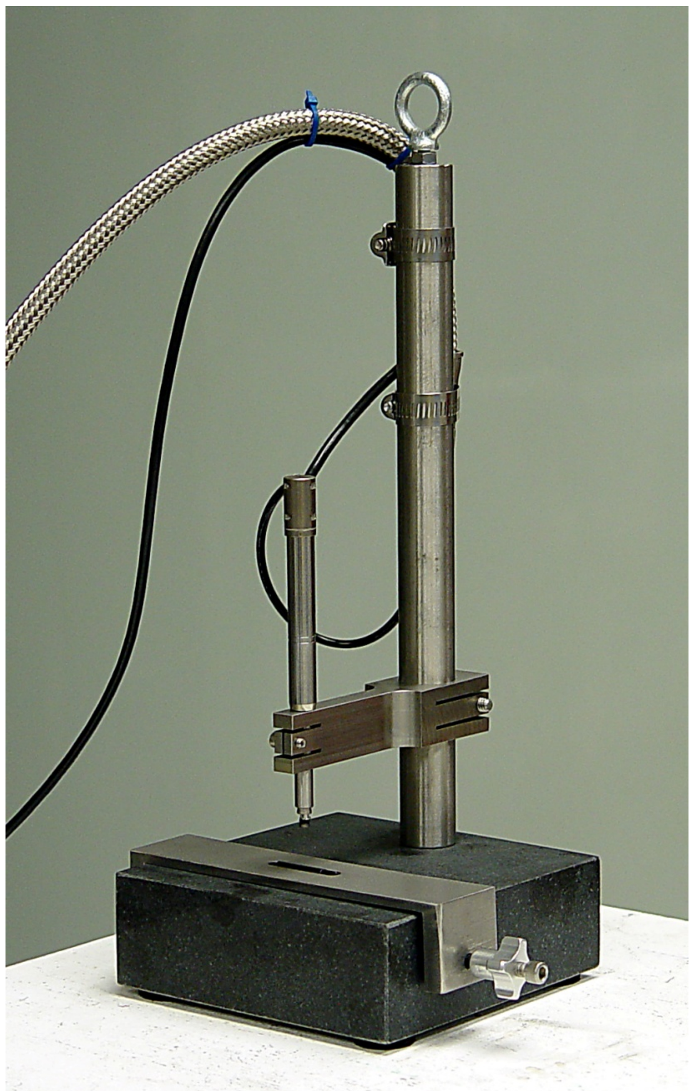

Fig. 4.17. Measurement sensor.

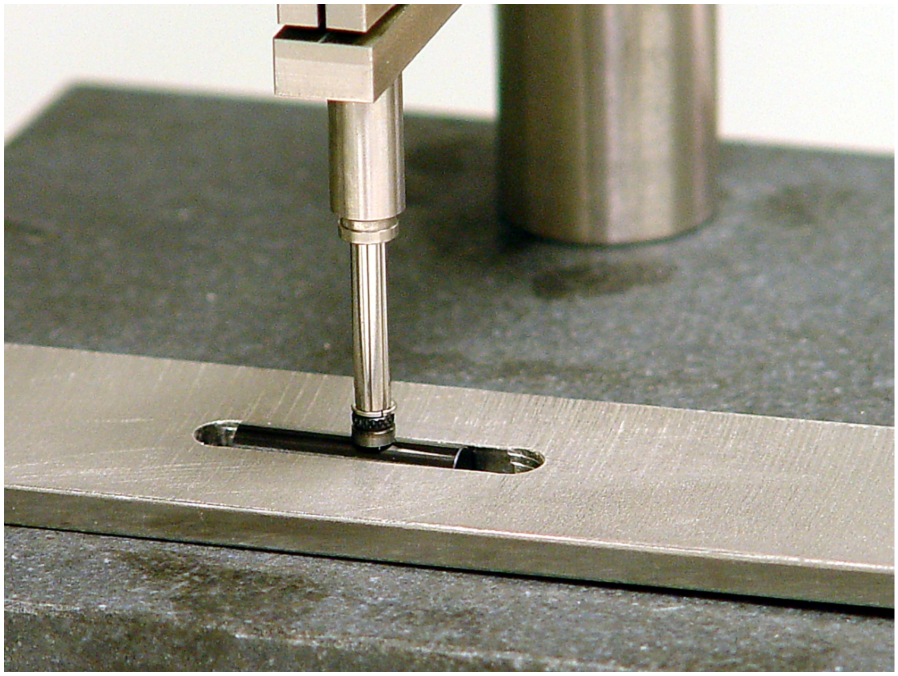

Fig. 4.18. Measurement probe contacting pin gauge (black item in slot).

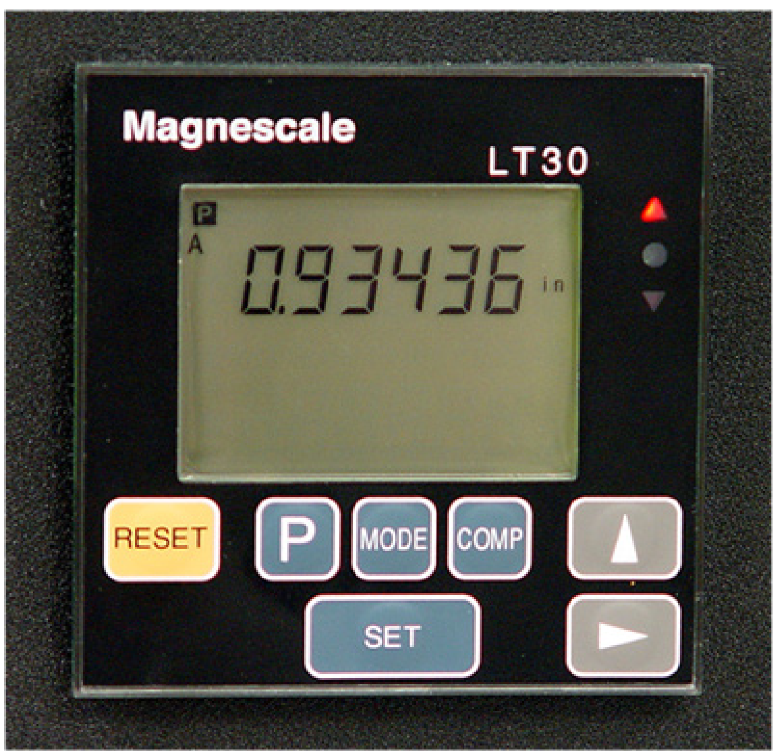

Fig. 4.19. Display of the measure sensor.

Table 4.3. Outer diameter measurement for as-fabricated and hydrided samples before the HFIR irradiation

Specimen ID	As-received, LRR4A27	Hydrided, UFC1D1A
First Measurement at 0°, in.	0.3730	0.3725
Second measurement at 0°, in.	0.3730	0.3720
First Measurement at 90°, in.	0.3730	0.3725
Second measurement at 90°, in.	0.3730	0.3725
Average	0.3730	0.3724

Table 4.4. Outer diameter measurement of the specimens from Capsule HYCD-1

Specimen ID	As-received LRR4A20	Hydrided LRR1B5
First measurement at 0°, in.	0.37346	0.37532
Second measurement at 0°, in.	0.37340	0.37524
First measurement at 90°, in.	0.37356	0.37578
Second measurement at 90°, in.	0.37352	0.37524
Average	0.37349	0.37540

Table 4.5. Outer diameter measurement of the specimens from Capsule HYCD-2

Specimen ID	As-received LRR4A23	Hydrided UFC1D1E
First measurement at 0°, in.	0.37324	0.37566
Second measurement at 0°, in.	0.37436	0.37544
First measurement at 90°, in.	0.37394	0.37530
Second measurement at 90°, in.	0.37394	0.37534
Average	0.37387	0.37544

5. ACKNOWLEDGMENTS

The authors wish to thank Dale Caquelin, Mark Delph, Rick Henry, Jeff Moody, Scott Thurman, and Bryan Woody for their help with hot cell operations and administration issues.

We would like to thank Josh Schmidlin for his help with the cladding OD measurements in the hot cell and Cliff Davison for his help with materials hydriding.

We wish to acknowledge the guidance and support of the program manager Rob Howard.

6. REFERENCES

1. M. Billone, Y. Yan, T. Burtseva, and R. Daum, *Cladding Embrittlement During Postulated Loss-of-Coolant Accidents*, NUREG/CR-6967, ANL-07/04, prepared for the U.S. Nuclear Regulatory Commission by Argonne National Laboratory, Argonne, IL, 2008.
2. R. Daum, H. Tsai, Y. Liu, and M. Billone, "High-Burnup Cladding Mechanical Performance During Cask Storage and Post-Storage Handling and Transportation," Nuclear Safety Research Conference, Washington, D.C., October 25-27, 2004.
3. M. C. Billone, T. Burtseva, Y. Yan, and S. Majumdar, "Overview of Spent Nuclear Fuel Program: Test Plan and High Burnup Cladding at ANL," NRC Program Review Meeting, Argonne, IL, July 7, 2010.
4. J. Huanga and S. Huanga, "Hydriding of Zirconium Alloys in Hydrogen Gas," *Mat. Sci. Eng. A* **161(**2), 247-253, April 1, 1993.
5. Y. Choi, J. W. Lee, Y. W. Lee, and S. I. Hong, "Hydride Formation by High Temperature Cathodic Hydrogen Charging Method and Its Effect on the Corrosion Behavior of Zircaloy-4 Tubes in Acid Solution," *J. Nucl. Mat.* **256**, 124-130, 1998.
6. Y. Yan, J. Kiggans, and C. Davisson, "Hydrogen Charging Techniques Being Developed at ORNL," DOE-UFC Clad Workshop, Las Vegas, NV, November 15-17, 2011.

APPENDIX A: DOSE RATE SURVEY REPORT ON HYCD-1 AND HYCD-2

ORNL Radiological Survey (3525-345245)

Survey Number:	3525-345245	**Survey Date:**	02/18/2013 1:42 PM
F Office:	3525	**Submitted Date:**	Not Submitted
Surveyor:	Allison Burnette (00963890)	**Approved Date:**	Not Approved
Surveyor (Other):	NA	**Survey Type:**	Other
Division / Group:	Nonreactor Nuclear Facilities Division	**RWP Number:**	3525-18367-7
Building:	3525	**Tickler Number:**	NA
Room:	130	**Person-Hours:**	1

Specific Location:
Charging Area, West Cell Port

Description:
Radiation and contamination survey in support of Dose Rating 2 HYCD Capsules.

Radiological Conditions:
The Charging Area was posted as a Controlled Area, Airborne Radioactivity Area, Radiation Area, and Contamination Area.

Dose rate at the threshold of the West Cell Port was 35 mrem/hr.
Work Area dose rates ranged from 0.5 to 685 mrem/hr.

The 2 HYCD capsules were raised to the West Cell Port using the in cell Manipulators to obtain dose rates.

Dose rates on the HYCD capsules were:

- UFC1D1C: 20 rem/hr at 1cm and 1 rem/hr at 30cm
- LRR1D7: 40 rem/hr at 1cm and 4 rem/hr at 30cm
- Note: Dose rates were taken using an Ion Chamber. The dose rates were taken at 1 cm per the researchers request.

Removable contamination levels after the dose rates were taken ranged from:

- <20 dpm/100cm^2 alpha
- <200 to 486 dpm/100cm^2 beta-gamma

Created by Allison Burnette (00963890) - Edited by Allison Burnette (00963890)

Instruments (8)

Instrument	Model	Next Calibration	Comments
0069461	ISOLO	09/30/2013	
M075758	3030	09/30/2013	
M133725	PORT	09/01/2013	Low Vol.
M133819	3030	09/30/2013	
M146622	RO-20	10/10/2013	
M146915	PAS	04/15/2013	
M146986	RadEye SX A/B	05/13/2013	
M147073	RadEye B20ER	04/22/2013	

COPY

Smears (3) (dpm/100cm2 unless noted)

Number	Alpha	Beta	Location
1	<20	486	Wall Under West Cell Port
2-(	<20	<200	Floor Under West Cell Port

Attachments (0)

APPENDIX B: HYDRIDED ZIRCALOY-4 AND ZIRLO SAMPLES FOR HFIR IRRADIATION

Assemble	Sample length (in.)	Materials	Hydrogen content (wppm)	Status	Comments
HYCD#1	3 × 1	Zry-4	20, 450, 820	Removed after 1 cycle	Feasibility testing (equiv. burnup: <10 GWd/MTU)
HYCD#2	3 × 1	Zry-4	20, 450, 550	Removed after 3 cycles	Provide a guideline for following tests (equiv. burnup: ≈20 GWd/MTU)
HYCD#3	6	Zry-4	770	Inserted into HFIR on 3/26/12 (to be removed Nov 2014 after 11 cycles)	Single 6 in.-long sample (equiv. burnup: ≥60 GWd/MTU)
HYCD#4	3 × 1	ZIRLO	15, 450, 460	Inserted into HFIR on 11/20/12 (to be removed Fall of 2014 after 11 cycles)	Multi 1-in. long samples (equiv. burnup: ≥60 GWd/MTU)
HYCD#5	3 × 1 + 3	Zry-4	20, 110, 280, 50	To be irradiated	Low H content to address hydride reorientation (equiv. burnup: TBD)
HYCD#6	6	Zry-4	440	To be irradiated	Single 6 in.-long sample having lower H content than HYCD#3 (equiv. burnup: TBD)

APPENDIX C: DRAWING X3E020977A608